Kinetics of Alkaline Activation of Slag and

Fly ash-Slag Systems

by

Sundara Raman Chithiraputhiran

A Thesis Presented in Partial Fulfillment
of the Requirements for the Degree
Master of Science

Approved September 2012 by the
Graduate Supervisory Committee:

Narayanan Neithalath, Chair
Barzin Mobasher
Subramaniam Rajan

ARIZONA STATE UNIVERSITY

December 2012

ABSTRACT

Alkali-activated aluminosilicates, commonly known as "geopolymers", are being increasingly studied as a potential replacement for Portland cement. These binders use an alkaline activator, typically alkali silicates, alkali hydroxides or a combination of both along with a silica-and-alumina rich material, such as fly ash or slag, to form a final product with properties comparable to or better than those of ordinary Portland cement.

The kinetics of alkali activation is highly dependent on the chemical composition of the binder material and the activator concentration. The influence of binder composition (slag, fly ash or both), different levels of alkalinity, expressed using the ratios of Na_2O-to-binders (n) and activator SiO_2-to-Na_2O ratios (M_s), on the early age behavior in sodium silicate solution (waterglass) activated fly ash-slag blended systems is discussed in this thesis.

Optimal binder composition and the n values are selected based on the setting times. Higher activator alkalinity (n value) is required when the amount of slag in the fly ash-slag blended mixtures is reduced. Isothermal calorimetry is performed to evaluate the early age hydration process and to understand the reaction kinetics of the alkali activated systems. The differences in the calorimetric signatures between waterglass activated slag and fly ash-slag blends facilitate an understanding of the impact of the binder composition on the reaction rates. Kinetic modeling is used to quantify the differences in reaction kinetics using the Exponential as well as the Knudsen method. The influence of

temperature on the reaction kinetics of activated slag and fly ash-slag blends based on the hydration parameters are discussed.

Very high compressive strengths can be obtained both at early ages as well as later ages (more than 70 MPa) with waterglass activated slag mortars. Compressive strength decreases with the increase in the fly ash content. A qualitative evidence of leaching is presented through the electrical conductivity changes in the saturating solution. The impact of leaching and the strength loss is found to be generally higher for the mixtures made using a higher activator M_s and a higher n value. Attenuated Total Reflectance-Fourier Transform Infrared Spectroscopy (ATR-FTIR) is used to obtain information about the reaction products.

To Appa, Amma, Akka, Athaan, Mahi and Jai

ACKNOWLEDGEMENTS

TABLE OF CONTENTS

LIST OF TABLES

LIST OF FIGURES

xiv

1. INTRODUCTION

As per the European Cement Association the global cement production in the year 2011 is approximately 3.2 billion. Cement manufacture results in significant amounts of CO_2 emissions. With the increased importance on sustainability the research on eco-friendly cements with fly ash and ground granulated blast furnace slag (GGBFS) has drawn global interest. 100% cement replacement in concrete can be achieved by alkali activation of alumino-silicate materials commonly referred to as Geopolymers. Most research is focused only with alkali-activation of fly ash or slag, however little information is reported on the combined use of both. The combination of fly ash and slag results in altering the chemical composition of the starting materials in order to develop beneficial properties that otherwise might not be possible. Thus this thesis focuses on explaining the influence of binder composition (fly ash, slag or both), activator solution concentration and curing conditions on the properties of slag and fly ash-slag blended systems. The influence of temperature on the kinetics of activation and hydration parameters is discussed through kinetic modeling. Detailed experimental studies have been conducted to understand the early age properties of the binder including its reaction kinetics and setting behavior. Reaction products formed in such systems have been characterized by means of advanced material characterization techniques. It is expected that an increased appreciation of the properties of these systems facilitated through this study would provide an impetus to the increased use of cement-free binder concretes.

1.1 Objectives

The two main objectives of this study are:

- To understand the early age behavior and the reaction kinetics of liquid sodium silicate (waterglass) activated slag and fly ash–slag blended systems.

- To understand the influence of early age response on the mechanical properties and the reaction product formation in fly ash rich binders and to determine the optimal alkalinity needed to activate them under ambient conditions, while maintaining reasonable mechanical properties.

1.2 Thesis Layout

Chapter 2 provides a literature review on alkali activated binder systems. It includes a review of the reaction mechanisms of alkali activated binders and their properties. It also includes a review of the different testing techniques used in the characterization of alkali activated binders. Chapter 3 presents the material properties, mixture proportions, mixing procedure and test methods used to evaluate the properties of alkali activated slag and fly ash-slag blended systems.

Chapter 4 details the early age behaviour and the reaction kinetics of waterglass activated slag and fly ash–slag blended systems. Setting time data is reported in this chapter that is used as a basis for identifying the optimal binder composition to be used for the isothermal calorimetric experiments. It also includes the isothermal calorimetry experimental procedure used to illustrate the influence of binder composition and the activator parameters on the reaction kinetics. The influence of temperature on the reaction kinetics of slag and fly ash rich blends

are also discussed in this chapter based on the hydration parameters. Finally, kinetic modeling is used to quantify the distinction in the reaction kinetics using different modeling methods and is compared to that of ordinary Portland cement hydration.

Chapter 5 discusses the influence of curing duration, binder composition and activator characteristics on the compressive strength. The optimal alkalinity needed to activate the fly ash rich binders under ambient curing conditions are determined. The influence of leaching on strength reduction of highly alkaline activated systems is shown based on electrical conductivity measurements of solutions in which the specimens were leached. The reaction product formation in fly ash rich binders is studied using analysis of the ATR-FTIR spectra. A brief study on the influence of curing conditions on the compressive strength and the reaction product formation of heat cured fly ash rich binders is also reported.

Finally, Chapter 6 provides a detailed conclusion of the studies carried out on alkali activated binder systems.

2. LITERATURE REVIEW

In this chapter the existing published work on the alkali activated fly ash, slag and other aluminosilicate materials as the binding medium is discussed. The early age properties of these materials are discussed along with the kinetics and chemical aspects of reaction product formation.

2.1 Background and Overview

Portland cement production increases global greenhouse gas emissions through the calcination of clinker in hydrocarbon heated furnaces. Traditionally, reduction in cement consumption has been attained by the use of industrial by products such as fly ash and ground granulated blast furnace slag (GGBFS) as partial cement replacement materials. Nowadays with the increasing importance on sustainability, researchers have tried to use industrial by-products such as fly ash and slag as the sole binding material in concretes instead of partial replacement of ordinary Portland cement. Alkali activated binder concretes, also known as geopolymer concretes is a result of this approach. Due to their excellent mechanical properties, the use of geopolymeric materials in construction is gaining importance. This class of materials was originally developed in France in the 1980's as the result of a search to develop new fire resistant building materials. In order to effectively apply these composites as engineering resources, it is essential to understand the properties, microstructure and performance characteristics of these materials. Numerous studies have been conducted over the last few decades to determine the composition-microstructure-property

relationships in such systems. This research will assist in a better understanding of the material and provide valuable information to adapt the material for specific applications in the infrastructure sector.

2.2 Historical Developments of Alkali Activated Cement and Concretes

Alkali was used as a component in the cementing material first by Kuhl (1930). He investigated the setting behaviour of mixtures of ground slag powder and caustic potash solution. Purdon (1940) did the first extensive laboratory study on cements consisting of slag and caustic alkalis produced by a base and an alkaline salt. Glukhovsky (1957) discovered that binders can be produced using calcium-free aluminosilicate and alkali metal solutions. He referred the binders as "soil cements" and the corresponding concretes as "soil silicates". Glukhovsky divided the binders into two groups: alkaline binding system $Me_2O–Me_2O_3–SiO_2–H_2O$ and alkaline earth alkali binding system $Me_2O–MeO–Me_2O_3–SiO_2–H_2O$ based on the composition of starting materials. In 1979, Davidovits developed a new type of binder similar to the alkaline binding system, using sintering products of kaolinite and limestone or dolomite as the aluminosilicate constituents. Davidovits (1991) adopted the term "geopolymer" to emphasize the association of this binder with the earth mineral found in natural stone. He stated that this type of materials virtually belongs to the alkaline binding system. Later, Krivenko (1994) pointed out the difference between use of alkali as an accelerator and alkali as a part of structure forming element in such systems.

5

2.3 Applications of Alkali Activated Binder Systems

Alkali activated binder systems have diverse applications. The commercial products developed using alkali activated binder systems include structural concrete, masonry blocks, concrete pavements, concrete pipes, utility poles and concrete sinks and trenches. It is also used in the development of autoclaved aerated concrete, refractory concrete and oil-well cements. Most of the commercial applications of this system have taken place in the former Soviet Union, China, and some Scandinavian countries. Alkali activated binder systems have been found to provide high strength and good durability characteristics. The system is found to show better fire resistance [Glifford and Gillot 1996, Bakharev 2005, Kumar et al 2006, Kong et al 2007], thus providing the potential to replace Ordinary Portland Cement concretes. Alkali activated concretes also have been used as repair materials due to their superior early age strengths (in most cases, depending on the activator and source material chemistry) and better bonding with the substrate material [Huet al. 2008]. Geopolymers are ideal for high temperature applications as they remain structurally stable at temperatures up to 800°C [Rashad and Zeedan 2011]. When combined with carbon fibers to form a composite material, geopolymers proved to be cost-effective when compared to traditional carbon fiber/resin composites and performed better in structural and functional applications including those at high temperatures [Lin et al. 2008]. The need for "green" technologies has also created applications for geopolymers in areas involving immobilizing toxic metals and reducing CO_2 emissions

[Yunsheng et al. 2007]. Other siliceous calcareous materials, such as red mud-slag [Gong and Yang, 2000, Pan, Cheng, Lu and Yang, 2002] and high-calcium fly ash can also be activated to form binding materials [Chindaprasirt et al. 2007], although not as effectively as slag. The application of alkali activated aluminosilicates mainly depends on the Si/Al ratio of the starting material. Table 2.1 shows the possible application of alkali aluminosilicate materials.

Table 2.1: Applications of alkali aluminosilicates [Bakharev 2006]

Si/Al	Application
1	Bricks, ceramics, fire protection
2	Low CO_2 cements, concrete, radioactive and toxic waste encapsulation
3	Heat resistance composites, foundry equipment, fiber glass composites
> 3	Sealants for industry
20<Si/Al<35	Fire resistant and heat resistant fiber composites

2.4 Alkaline Activators

Fly ash, slag and other alumina silicate materials need to be activated using alkalis to form the resulting binding material. Typically, caustic alkalis or alkaline salts are used as alkaline activators. Table 2.2 shows the classification of alkali activators into six groups according to their chemical compositions.

Table 2.2: Classification of Alkali activators [Glukhovsky et al. 1980]

Alkali Activator	Chemical Formula
Hydroxides	MOH
Non-silicate weak acid salts	$M_2CO_3, M_2SO_3, M_3PO_4, MF$
Silicates	$M_2O \cdot nSiO_2$
Aluminates	$M_2O \cdot nAl_2O_3$
Aluminosilicates	$M_2O \cdot Al_2O_3 \cdot (2–6)SiO_2$
Non-silicate strong acid salts	M_2SO_4

M - Metal

7

This section provides details on the alkali hydroxides and silicates used as activators.

2.4.1 Alkali hydroxides

Chemical compounds composing of an alkali metal cation and the hydroxide anion (OH^-) are called alkali hydroxides. They are the most widely used as activating agents. Sodium and potassium hydroxides are the most commonly used alkali hydroxides in the production of alkali activated binders. NaOH is reasonably cheap when compared to KOH and largely available making it an obvious pick for activation of alumina silicate materials. The use of high concentrations of NaOH or KOH as the activating agent has been reported to lead to the formation of zeolitic structures after an extensive period of moist curing or a brief period of heat curing. The dilution of NaOH releases a large amount of heat, thus requiring special precautions to be taken. The carbonation and leaching of the reaction products activated using the alkali hydroxides is a concern due to the high alkalinity in the system; so there is a need to identify the optimal alkalinity when using alkali activated systems which is also one of the main objectives of this work.

2.4.2 Alkali silicates

Sodium silicate is a very common alkali silicate used as activating agent for alkali activated binder systems. Sodium silicate is the generic name for a series of compounds with the formula $Na_2O \cdot nSiO_2$. Theoretically, the ratio n can be any number. Sodium silicates with different n have different properties that may have

many diversified industrial applications. Sodium silicates are available in solid as well as in liquid form. Liquid sodium silicates are commercially termed as waterglass. Solid sodium silicate consists of a chain of polymeric anions composed of corner shared $[SiO_4]$ tetrahedral. Different grades of sodium silicate are generally characterized by their silica modulus (SiO_2-to-Na_2O (or K_2O) ratio), which varies from 1.6 to 3.3. Commonly available waterglass has a silica modulus of 1.60 to 3.85 and contains 36-40% solids. It has been reported that waterglass are the most effective activators for most alkali-activated cementing materials [Shi and Li 1989a, b]. NaOH is often added to a sodium silicate solution to lower the silicate modulus to a more desired value. This method allows production of waterglass of the optimal modulus and concentration directly. The major difference between sodium and potassium silicates as far as their properties are concerned is the viscosity. Potassium silicate solutions have a markedly lower viscosity than sodium silicate at the same silica modulus, thereby making mixtures workable at a lower activator-to-binder ratio. However, potassium silicates are more expensive making them less conducive for practical applications.

2.5 Alkaline Activation of Aluminosilicate Based Binders

2.5.1 Source materials

The source materials used for making geopolymers based on aluminosilicates should be rich in silicon (Si) and aluminium (Al). There are three different models for alkali activated cements. The first type is obtained by the alkali activation of

9

materials comprising primarily of aluminium and silicon with low-calcium contents. An example of this is the alkali activation of Class F fly ash or metakaolin. In this case more severe conditions (high alkalinity and curing temperatures from 60 to 200 ºC) are required. The main reaction product formed in this case is a three-dimensional alkaline inorganic polymer, an alkaline aluminosilicate gel that can be regarded to be a zeolite precursor (Palomo et al 1999, Palomo et al. 2004, Duxson et al. 2007). The second type is obtained by the alkali activation of calcium and silicon rich materials such as ground granulated blast furnace slag. In this case the main reaction product is a calcium silicate hydrate or C-S-H gel (Fernández-Jiménez 2000, Shi et al 2006), similar to the gel obtained during Portland cement hydration. A third group of materials has recently come to the attention of researchers and may prove to be of particular interest to the construction industry. This group is the result of alkali activating a blend of the previous two, i.e., a Ca, Si and Al rich (Yip et al. 2005, Palomo et al. 2007a) material.

2.5.2   *Aluminosilicate structure and nomenclature*

The molecular structures of geopolymers are identified by the term polysialate. The term was coined as a descriptor of the silico-aluminate structure for this type of material. The network is configured of SiO_4 and AlO_4 tetrahedrons united by oxygen atoms (Figure 2.1) [Davidovits 1999]. Due to the negative charge of the Al tetrahedral in IV-fold coordination, positive ions must be present to balance out this charge. Positive ions (Na^+, K^+) must compensate the negative charge

which is the reason why alkalis are used as the activating agents. SiO_4 structural units can be classified into seven types: Q^0, Q^1, Q^2cy–3, Q^2, Q^3cy–3, Q^3 and Q^4. [Shi et al., 2006]. The superscripts on the Q represent the number of linkages between the given Si atom and neighbouring Si atoms by =Si–O–Si= bonds. The symbols Q^2cy–3 and Q^3cy–3 represent intermediate or branched SiO_4 structural units.
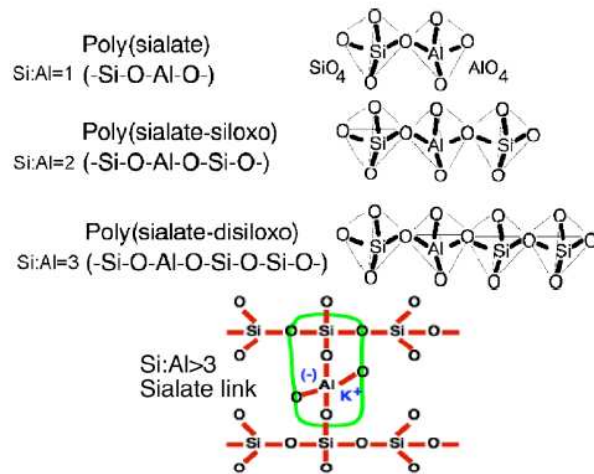
Figure 2.1: Aluminosilicate Structure [Davidovits 2005].

2.5.3 Geopolymerization process

The geopolymerization process is an exothermic polycondensation reaction involving alkali activation by a cation in solution. The reaction leading to the formation of a polysialate geopolymer is shown below: [Davidovits 1999]

$$(Al_2Si_2O_7)_n + nH_2O \xrightarrow{MOH} n(OH)_3 - Si - Al - (OH)_3 \qquad 2.5.3.1$$

$$n(OH)_3 - Si - O - Al - (OH)_3 \xrightarrow{MOH} M\left(\begin{matrix} | & | \\ -Si - O - Al^{(-)} - O \\ | & | \\ O & O \end{matrix} \right)_n + nH_2O \qquad 2.5.3.2$$

11
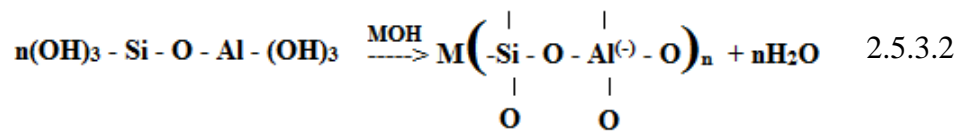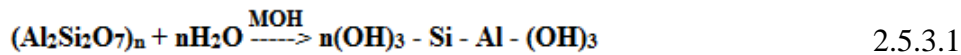
In the above equations, M is the cation used to activate the reaction which is typically introduced as either KOH or NaOH. Additional amounts of amorphous silica must be present in order to form either the polysialate-siloxo or polysialate-disiloxo structures of geopolymers. The reaction for the polysialate-siloxo formation is also provided below as an illustration of how the two reactions differ [Davidovits 2005]. After the geopolymerization process is completed, the final geopolymer obtained is described by the empirical formula:

$$M_n\{-(SiO_2)z-(AlO_2)\}n + H_2O$$
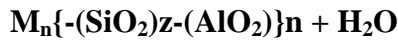
Here M again is a cation used to activate the reaction, n is the degree of polycondensation, and $z = 1, 2, 3$ for polysialate, polysialate-siloxo, and polysialate-disiloxo structures respectively. The step-wise reaction is shown in Figure 2.2
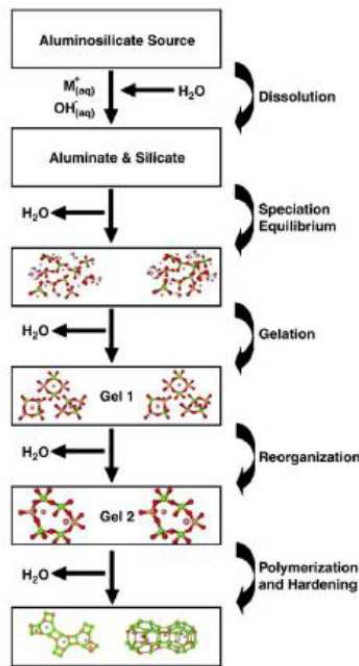
Figure 2.2: Geopolymerization process [Duxon et al. 2007]

2.5.4   Alkali activation of fly ash

Fly ash is a by-product of coal combustion, generally captured by electrostatic precipitators before the flue gases reach the chimneys of thermal power plants. It is the preferred supplementary cementitious material and has extensively been used to replace part of cement in concrete. Unused fly ash is usually disposed into landfills contributing to soil, water and air pollution [Palomo et al 1999, Duxon et al. 2007]. Fly ash is usually classified as low-Ca fly ash or Class F fly ash and high Ca fly ash or Class C fly ash. Class F fly ash is generally preferred for synthesis of geopolymer concretes due to the high availability of reactive silica and alumina. Alkali activation of fly ash takes place through an exothermic reaction with dissolution during which the covalent bonds (Si-O-Si and Al-O-Al) in the glassy phase pass through the solution.
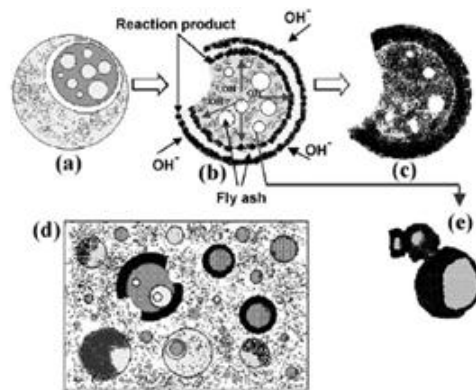
Figure 2.3: Mechanism of Gel formations in alkali activated
fly ash binder [Jimenez et al 2005]

The products generated from dissolution start to accumulate for a certain period of time (called the induction period) during which the heat release is really low.

13

Isothermal calorimetric studies (explained in a forthcoming section) are used to distinguish the extent of the induction period in systems proportioned using different activator and binder types, concentration, and dosages. A condensation of the structure is produced (a highly exothermal stage), which involves the creation of a cementitious material with a poorly ordered structure, but high mechanical strength. The product is an amorphous alkali aluminosilicate gel having a structure similar to that of zeolitic precursors. This formation of reaction product as a layer around the fly ash particles is explained as the mechanism of geopolymerization and is depicted in Figure 2.3 below. Most research reveals that the activation of fly ash with alkalis requires heat curing to gain reasonable mechanical properties. The type of solution used for the activation of the fly ash is essential in the development of reactions. When the alkali solution contains soluble silicates (sodium or potassium silicate), the reactions occur at a higher rates than when hydroxides are used as the activators.

2.6 Alkaline Activation of Slag

2.6.1   Reaction mechanism

The reaction mechanism of aluminosilicates containing a calcium bearing compound differs from the geopolymeric reaction as explained in the previous section. It has also been reported that the type of calcium bearing compound in the starting material also play an important role in the alkali activation of such materials. An example of such is the alkali activation of slag. Alkalis first attack the slag particles breaking the outer layer and then a polycondensation of reaction

products takes place. Wang et al. (2004) suggested that though the initial reaction products form due to dissolution and precipitation, at later ages, a solid state mechanism is followed where the reaction takes place on the surface of the formed particles, dominated by slow diffusion of the ionic species into the unreacted core. Alkali cation (R^+) acts as a mere catalyst for the reaction in the initial stages of hydration as shown in the following equations, via cation exchange with the Ca^{2+} ions [Glukhovsky, 1994 and Krivenko, 1994].

=Si-O- + R$^+$ → =Si-O-R

=Si-O-R + OH- → =Si-O-R-OH$^-$

=Si-O-R-OH- + Ca^{2+} → =Si-O-Ca-OH + R$^+$
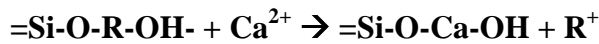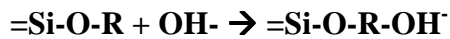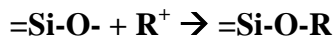
The alkaline cations act as structure creators. The nature of the anion in the solution also plays a determining role in activation, particularly in early ages and especially with regard to paste setting (Fernández-Jiménez and Puertas 2001, Fernández-Jiménez and Puertas 2003).

The descriptive model is shown in Figure 2.4. The final products of the slag reaction are similar to the products of cement hydration (C-S-H); the major difference being the rate and intensity of the reaction. Slag also exhibits pozzolanic activity in the presence of calcium hydroxide [Mindess et al. 2003]. Therefore a mixture of Portland cement and slag will have at least three component reactions; cement hydration, slag hydraulic reaction, and slag pozzolanic reaction [Feng, et al. 2004]. It has also been observed that the alkalis are bound to the reaction products and are not freely available in the pore solution

(this depends on the alkali concentration used, though), thereby negating the potential for alkali-silica reactivity. Drying shrinkage of alkali-slag cement pastes is reported to be considerably higher than that of Portland cement pastes [Krizan and Zivanovic 2001].
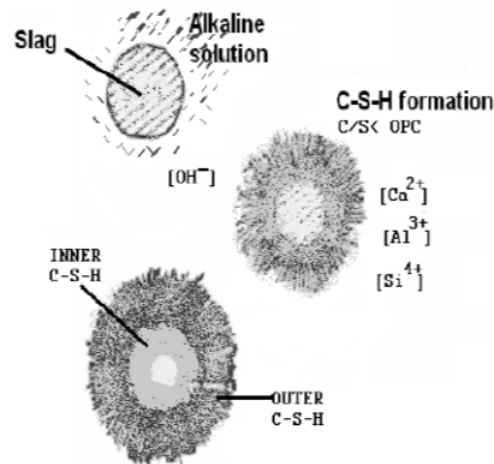
Figure 2.4: Reaction mechanism of alkali activated slag [F Jimenez 2000]

Figure 2.5 shows the concept mapping of the likely products resulting from the alkaline activation of alumina silicates in the presence of a calcium source.
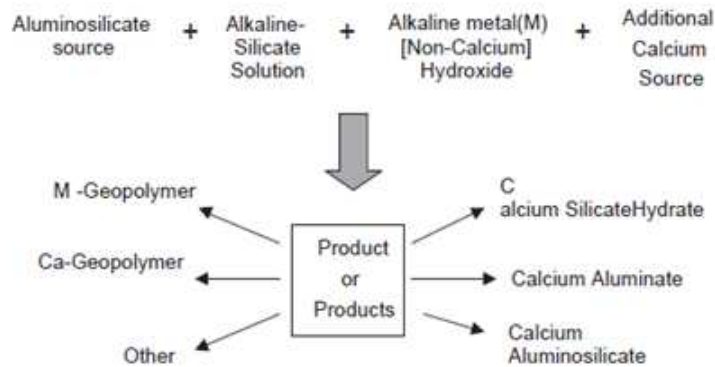
Figure 2.5: Concept mapping of the reaction products [Yip et al 2005]

2.7 Alkaline Activation of Aluminosilicate Blended Binders

2.7.1   Alkali activation of fly ash-slag systems

Fly ash-slag blends are chosen to obtain inexpensive, low energy, and environmentally friendly materials. By combining both the materials the disadvantages of one activation process can be balanced by the advantages of the other one. In fly ash-slag blended systems the early age strength has shown to be decent, however it displayed very little strength gain beyond 28 days. Strength improvements may be obtained by varying fly ash-slag ratios or by increasing the fineness of the slag [Smith and Osborne 1977]. The fly ash-slag ratio has remarkable influence on the mechanical strength of the cementing material. As slag content in the pastes increases, compressive strength increases. The addition of a little amount of hydrated lime considerably increases the early-age strength but slightly decrease the later-age strength of the activated fly ash-slag blends [Shi and Day 1999]. The strength also increases with increased alkalinity. The mechanical strength development of the fly ash-slag pastes activated with NaOH solutions is found to be affected more by the fly ash-slag ratio and the activator concentration [Puertas et al 2000]. At 28 days of reaction, a mixture of 50% fly ash-50% slag activated with 10 M NaOH solution and cured at 25°C develops compressive strengths higher than 50 MPa. When NaOH was used as an activator, the slag blended with Class F fly ash or with Class C fly ash did not show a significant effect on strength development. Both fly ashes had a significant effect on the strength development when powdered sodium silicate was used as an

activator. Proper amount of fly ash can reduce the cost and without negative contribution to the flexural strength. The fly ash-slag blended cements carbonated much faster than pure slag cement and OPC. Carbonation of these materials leads to micro cracking which in turn reduces the strength [Bijen and Waltje 1989]. The present study is mainly concerned with the influence of binder composition, activator parameters (n and M_s) and temperature on the reaction kinetics of waterglass activated fly ash-slag blended systems.

2.8 Synthesis of Alkali Activated Binders

Production of cement free binder concrete needs an alumino silicate rich material as the binder, alkali for activation and in certain cases heat curing to attain reasonable mechanical properties. The silicon and aluminium oxides in the source material react with the alkaline liquid to form the geopolymer paste.

2.8.1   Curing conditions

Different types of curing methods are employed, such as moist curing, heat curing (low (more than ambient) and at very high temperatures up to 800°C), and steam curing. These curing methods can also be combined, for example, heat curing during the initial few hours and then placed under moist curing [Puertas et al. 2000] for the remaining duration to determine the strength at various ages. Activation of aluminosilicate materials with alkalis generally requires heat curing for the formation of alkali aluminosilicate binders. A wide range of temperatures ranging from 40^oC to 90^oC have been reported in order to produce alkali activated binders with considerable mechanical properties [Hardjito and Rangan 2005] with

18

a general improvement in mechanical properties when higher temperatures are used. Alkali activation of aluminosilicates without the presence of a Ca-bearing compounds certainly need heat curing to obtain requisite mechanical properties. Hence, one of the objectives of this study is to identify the optimal alkalinity required to activate fly ash rich blends under ambient curing conditions. Alkali activated slag concretes can be moist cured owing to the potential for the formation of calcium silicate hydrates (C-S-H) as the reaction product, as explained earlier. Prolonged heat curing leads to shrinkage and consequent cracking and thus curing duration and temperature is dependent on the type of binder and activator used. The start of heat curing of the geopolymer concrete can be delayed for several days. Tests have shown that a delay in initiation of heat-curing up to five days did not produce any degradation in the compressive strength. In fact, such a delay in the start of heat-curing substantially increased the compressive strength of geopolymer concrete. The above flexibilities in the heat-curing regime of geopolymer concrete can be exploited in practical applications. Curing temperature has a positive effect in the strength increase at the early days of reaction. At later ages, the effect is reversed and strengths are higher when curing temperature is low. The influence of curing temperature in the development of the strength of the pastes is low compared to the influence of other factors such as the ratio of fly ash-slag and the activator concentration [Puertas et al 2000]. If all other factors remain constant, the temperature increase tends to result in a gain of mechanical strength. [Paloma et al 1999]. Thus the

temperature and time of curing significantly affects the strength in the case of alkali activated fly ash. A study on the effects on curing conditions (sealed (using aluminium foil) and open (dry and moist) on the compressive strength development of heat cured fly ash systems are shown in Chapter 5.

2.9 Properties of Alkali Activated Binders

2.9.1 Early age properties

Setting time is one of the early age property of cementitious systems. The setting times of alkali-activated slag cement pastes depend on the nature of activators. NaOH and Na_2CO_3 activated slag cement pastes usually exhibited longer setting time than waterglass activated slag cements. The setting times usually decrease with the increase of activator dosage. The modulus of sodium silicate has a very significant effect on the setting times of sodium silicate-activated slag cements (Shi and Li 1989a, b, Bakharev et al. 1999a). Both the initial and final setting times of the pastes decrease with the increase in the silicate modulus when waterglass (liquid sodium silicate) is used [Cheng 2003]. Figure 2.6 shows the influence of activator dosage and silicate modulus on the setting time of waterglass activated slag. However when solid silicate is used the setting time increases with the increase in the silicate modulus. This is because both the dissolution rate and solubility of sodium silicate glasses decrease as the modulus of the solid sodium silicate increases
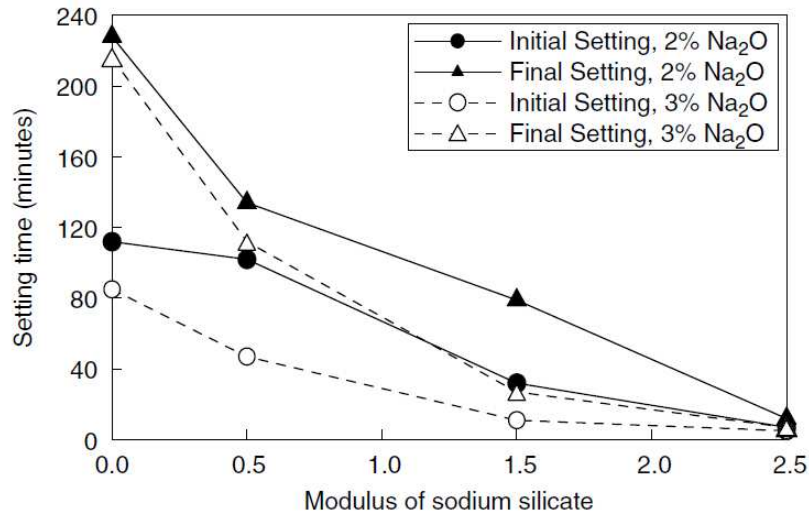
Figure 2.6: Effect of alkali dosage and silicate modulus on setting times of alkali-
activated slag (Shi and Li 1989b)

Hydration is another important early age property of cementitious materials.
Ordinary Portland cement hydration is usually a five stage process, as shown in
Figure 2.7. The first stage is the initial dissolution (pre-induction stage) of cement
grains when water is added. This stage is typically no more than few minutes.
Following this is the dormant period (induction stage), in which the rate of
reaction slows down significantly. This dormant period typically lasts for a few
hours and allows for the transportation and placement of the mix. After this
induction stage is the acceleration stage, where the rate of hydration accelerates
rapidly and reaches a maximum within about 5-10 hours. The acceleration of the
reaction is due to the formation of reaction products (C-S-H) [Shi 1999]. Post-
maxima the rate of hydration slows down gradually (deceleration and long-term

21

hydration stages), with the long-term hydration process being diffusion controlled.
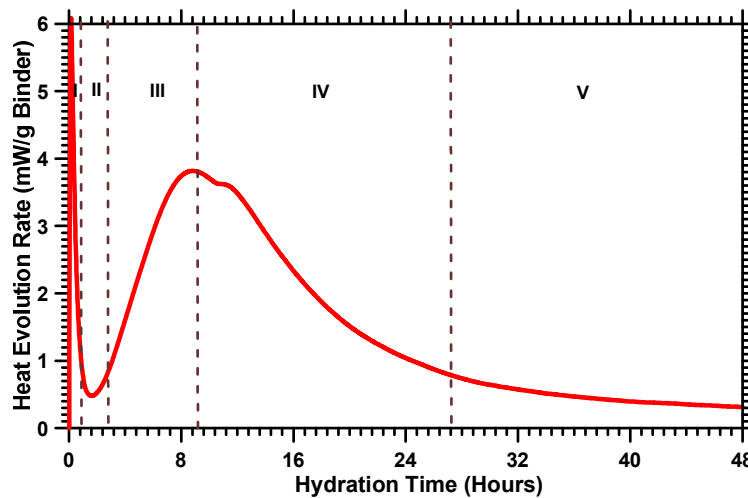
Figure 2.7: Rate of heat evolution during the hydration of OPC

In alkali activated slag, the reaction product is predominantly C-S-H with low Ca/Si ratio. The reaction kinetics is influenced by the activator type, temperature and alkalinity of the activator. In waterglass activated slag a similar heat release response as seen for ordinary Portland cement hydration is observed as shown in Figure 2.8. The heat evolution peaks appears to be directly proportional to the alkali concentration and the time at which the heat evolution occurs decreases with alkali concentration. The cumulative heat of hydration increases by increasing the n modulus as well as the dosage of waterglass, but is still lower than that of Portland cement [Krizan and Zivanovic 2001]. It was found that the initial pH of activator solution has an important role in dissolving the slag and in promoting the early formation of some hydration products. The hydration of alkali-slag cements can be described by three models. The first model consists of

22

the case where there is only one initial peak and no further peaks. The second

model includes one peak before the induction period and one peak after the

induction period, and finally the third model includes two peaks before the

induction period and one peak after the induction period. [Shi and Day 2004]. For

NaOH activated slag the reaction takes place so quickly that the dissolution peaks

are not captured. Figure 2.9 illustrates the reaction kinetics of alkali activated slag

activated with NaOH. Temperature has a major influence on alkali activated

systems. The reaction kinetics of fly ash rich blends is a complicated process

since the fly ash particles reaction is accelerated only at higher temperatures.

There is not much research that has been done in the case of blended alkali

activated systems which is the focus of this research.
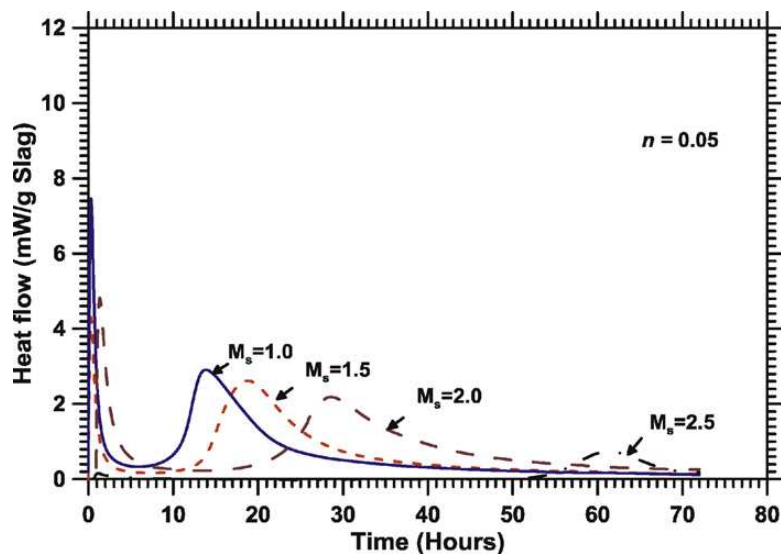
Figure 2.8: Calorimetric response of waterglass activated slag showing similar
calorimetric response to that of OPC hydration [Ravikumar and Neithalath 2012]
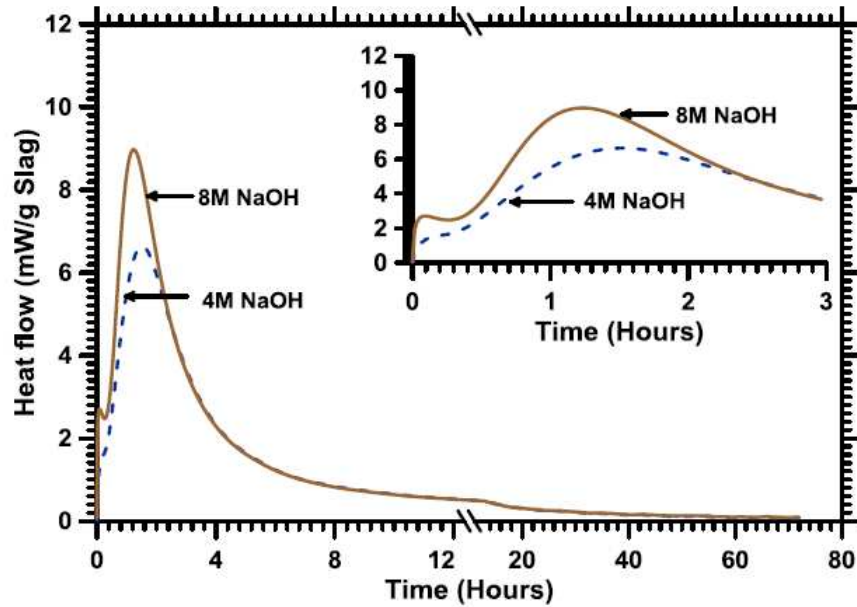
Figure 2.9: Calorimetric response of NaOH activated slag paste at different NaOH concentrations [Ravikumar and Neithalath 2012]

2.9.2 *Mechanical behavior*

Compressive strengths of alkali activated systems vary mainly because of the binders and the activators used. Concrete beams and columns made with activated fly ash have been tested for flexural and compressive strength and are reported to perform similar to or better than concretes produced with OPC. This might also be due to the better bonding of the reaction product with the aggregates. It has been proposed that the similar mechanical response could facilitate the use of similar structural design codes for alkali activated concretes as that currently exists for OPC concretes [Rangan et al. 2005]. Further study is required to learn the influence of binder composition and activator composition on the mechanical behaviour, of this new material. Limited studies on compressive behaviour of alkali activated fly ash concrete shows a similar compressive behaviour as that

24

seen for ordinary Portland cement concrete [Hardjito et al. 2005]. The modulus of elasticity of alkali activated slag concrete was in good agreement with that predicted from the equation specified in ACI 318-2011, however it was found that the alkali activated slag concretes had lower tensile capacity than those predicted from models for ordinary concretes [Yang et al. 2012].

2.9.3   Reaction products and microstructure

Fourier Transform Infra-Red (FTIR) Spectroscopy is an easy and quick method for analysis of reaction products in alkali activated binder systems. In infrared spectroscopy, infrared radiation is passed through a sample, where some of the radiation is absorbed and some transmitted. The resulting spectrum represents the molecular absorption and transmission, creating a molecular fingerprint of the sample. This makes infrared spectroscopy useful for identification of reaction products in these systems. Table 2.3 shows the common FTIR spectra peaks identified from literature for OPC and alkali activated pastes.

Table 2.3: Attributing FTIR peak signals to typical bonds [Yu et al. 1999]

Peak location (cm$^{-1)}$)	Chemical bond characteristic of the signal
3650	Hydrated Minerals (i.e. $Ca(OH)_2$)
3400	OH Stretching (H_2O)
1650	S-O (Gypsum) H-O-H Bending (H_2O)
1430	C-O Asymmetric Stretching
1035-1030	aluminosilicate bonding'
1010-1000	Calcium Silicates
960-800	Si-O, Al-O Stretching
872	C-O Bending
480	Si-O-Si and O-Si-O Bending

2.10   Summary

This chapter reviewed previous studies conducted on alkali activated systems. The background information was used to help in the design, interpretation, and analysis of the experimental data. Hence, the discussions in this thesis build on many of the research referenced in this chapter.

3. MATERIALS AND EXPERIMENTAL METHODS

This chapter describes the materials and methodology employed in the research presented in this thesis. The experimental methods used to make the samples are also explained in detail in this chapter along with a description of the analytical equipment employed.

3.1 Materials

The source materials used in this study are Class F fly ash conforming to ASTM C 618 and ground granulated blast furnace slag (GGBFS) Type 100 conforming to ASTM C 989, the chemical compositions of which are shown in Table 3.1. The reactivity of these materials, when activated with alkalis depends mainly on the CaO, SiO_2 and Al_2O_3 content of the binders. Figure 3.1 shows the CaO-SiO_2-Al_2O_3 ternary diagram indicating the location of the source materials.

Table 3.1: Chemical composition and physical characteristics

Chemical Analysis	Class F Fly ash	Slag
Silicon Dioxide (SiO_2)	57.96%	39.44%
Aluminum Oxide (Al_2O_3)	23.33%	6.88%
Iron Oxide (Fe_2O_3)	4.61%	0.43%
Calcium Oxide (CaO)	5.03%	37.96%
Sulfur Trioxide (SO_3)	0.39%	2.09%
Loss on Ignition (L.O.I)	0.45%	3.00%
Sodium Oxide (Na_2O)	1.28%	1.67%
Others	6.95%	8.53%
Density (g/cc)	2.28	2.9

Both these binding materials are rich in silica and alumina, which are required for the formation of the strength imparting phases in alkali activated binders. The silica-to-alumina (SiO_2/Al_2O_3) ratios were found to be approximately 2.48 and 5.73 for fly ash and slag respectively. Apart from the high silica and alumina contents, slag also has a high CaO content (~38%) while the CaO content in fly ash is very low (5.03 %).
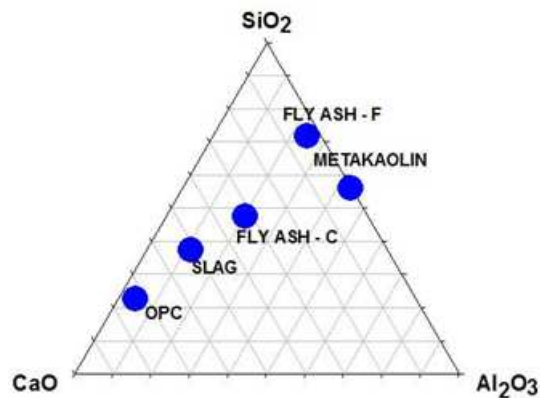
Figure 3.1: CaO-SiO_2-Al_2O_3 composition of different materials
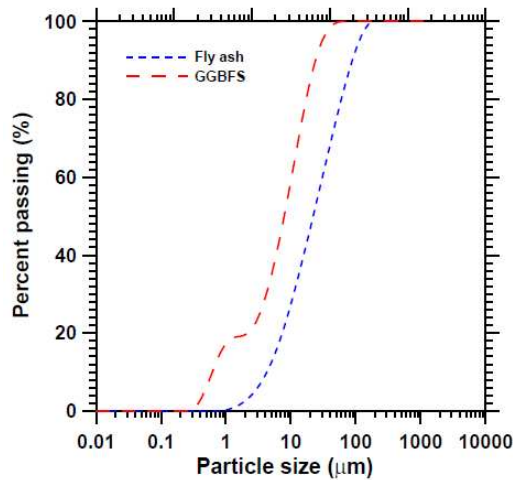
Figure 3.2: Particle size distribution of fly ash and slag [Ravikumar, 2012]

The particle size distributions (obtained using a laser particle size analyzer) are shown in Figure 3.2. Particle size analysis shows that slag is finer than fly ash with 95% of particles finer than 30 μm compared to only 60% for fly ash. Fly ash and slag particle morphologies obtained using scanning electron microscopy is shown in Figure 3.3 (a) and (b) respectively. Fly ash has smooth spherical particles whereas slag is composed of angular particles of varying sizes.

(a)   (b)
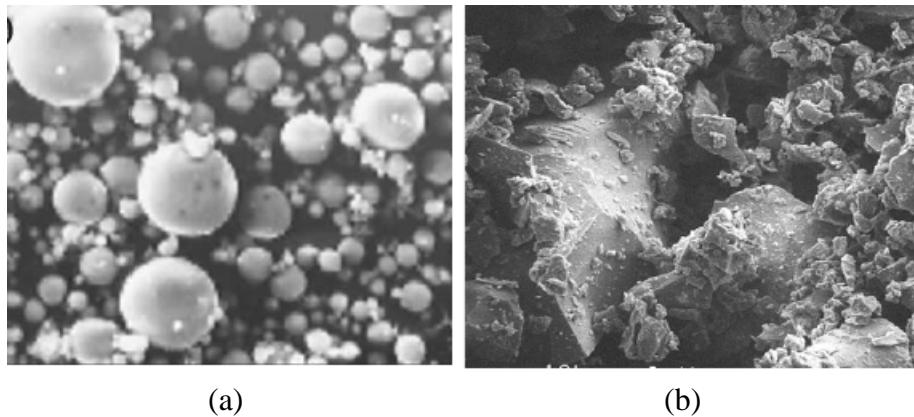
Figure 3.3: Scanning electron micrograph of a) Fly ash b) Slag (PCA 2000)

3.2 Activator Parameters (n and M_s)

The activator parameters that were chosen to be studied are the Na_2O-to-binder ratio (n) and the SiO_2-to-Na_2O ratio (also called the silica modulus, M_s). Binders are fly ash, slag, or both in the case of fly ash–slag blends. Sodium silicate solution (waterglass) is used as the activating agent, with a M_s ratio of 3.26. NaOH was added to the waterglass solution to adjust the M_s values as desired for beneficial activation. The ratio n provides the total amount of Na_2O in the mixture whereas the ratio M_s dictates the proportion of NaOH and sodium silicate solution

in the activator. The total alkali content in the mixtures were adjusted using the Na_2O-to-total source material content ratios (n), several values of which were used for activation, depending on the source material combination. For example, if a mixture with an n-value of 0.05 and a Ms of 1.5 is required, for every 1000 g of binders, 50 g of Na_2O and 75 g of SiO_2 is required. Since waterglass is the only source of silica from the activator, 75 g of SiO_2 can be obtained from 245 g of waterglass containing 98g of sodium silicate powder which has a M_s of 3.26. The waterglass would also provide 23 g of Na_2O. The remaining 27 g of Na_2O (50g – 23g) is then obtained by the addition of NaOH. Table 3.2 shows the mixture a proportion calculation for n values of 0.05 and 0.1 for three different M_s (1, 1.5 and 2) for 1000g of binders and a liquid-to-powder ratio of 0.5. The liquid consisted of the water added (a part of which was used to prepare the NaOH solution) and the water present in waterglass. The powder part consisted of the binders (fly ash, slag, or both), solid fraction of waterglass and Na_2O from NaOH.

Table 3.2: Sample Mixture Proposition

n	M_s	Binders (g)	Waterglass (g)	NaOH (g)	Water (g)
	1	1000	163	45	332
0.05	1.5	1000	245	35	295
	2	1000	327	25	258
	1	1000	327	90	264
0.1	1.5	1000	490	70	190
	2	1000	653	50	117

3.3 Mixing Procedure

The NaOH solution used to reduce the activator M_s was prepared by dissolving in water and added to the required amount of water glass. The resulting solution was then allowed to cool down to the room temperature for about 2 hours. The binders (fly ash, slag, or both) were first dry mixed together in a laboratory mortar mixer. The prepared activators are then mixed with the starting materials to prepare pastes. For mortars, fine aggregate (sand) was added to the source materials to obtain a 50% sand volume before the activators were added. They were mixed in a laboratory mixer for approximately 2 minutes until a homogeneous mixture is obtained. The mixtures were then cast in 50 mm cube molds for compressive strength testing. For the calorimetric and setting time studies, paste mixtures were used as soon as they were prepared. The liquid-to-powder ratio of 0.40 and 0.50 were used.

3.4 Early Age Tests

3.4.1 Setting time

The initial and final setting times of alkali activated pastes were determined using the method prescribed in ASTM C191 (Vicat needle method). Figure 3.4 shows the Vicat needle that has been used for determining the setting times.

Figure 3.4: Vicat Needle

3.4.2 *Isothermal Calorimetry*

Isothermal calorimetry has been shown to be a useful technique to study the hydration of cementitious systems [Wadsö, 2003], particularly during the first 72 hours of hydration. Isothermal calorimetry has the advantage of being able to test a material at a specific temperature. Typically, isothermal calorimetry is used to investigate the major thermal peak that occurs during the acceleration phase of the hydration process. The experiments were carried out in accordance with ASTM C 1679. Sodium hydroxide (NaOH) was mixed in water and allowed to cool to ambient temperatures. It was then mixed with sodium silicate solution (waterglass) to form the activator of desired M_s. The pastes were mixed externally and loaded into the isothermal calorimeter. The time elapsed between the instant the activating solution was added to the powder and the paste loaded into the calorimeter was around 2 minutes. This method of mixing was employed to avoid the large instantaneous heat release associated with alkali dissolution in water.

The tests were run for 72 hours with the calorimeter set at three different temperatures (25°C, 35°C, and 40°C).

Figure 3.5: Isothermal Calorimeter

In the cases where temperatures different from the ambient temperature were used for isothermal calorimetric experiments, requisite amounts of the source materials and the activator were placed inside the calorimeter chamber without being mixed for an extended duration (typically overnight) so as to equilibrate at the desired temperatures. Figure 3.5 shows the isothermal calorimeter used for this study.

3.5 Hardened Mortar Tests

3.5.1 Determination of Compressive Strength

The compressive strengths of the pastes and mortars were determined in accordance with ASTM C 109. The compressive strengths of the waterglass activated cubes at several ages were determined by testing at least three specimens from each mixture at the desired ages. Heat cured cubes were let to cool down over night before testing. Moist-cured specimens were tested at the respective ages without any drying.

3.6 Test Conducted to Quantify Leaching

3.6.1   Electrical Solution Conductivity

In order to quantify the leaching effects in alkali activated pastes, the cubes were placed in 300 ml of deionized water for an extended period of time. Electrical conductivity measurements of the deionized water in which the alkali activated specimens were stored for several days were conducted. Figure 3.6 shows the conductivity meter (Mettler Toledo) used to measure the conductivity of the solution containing the sample.
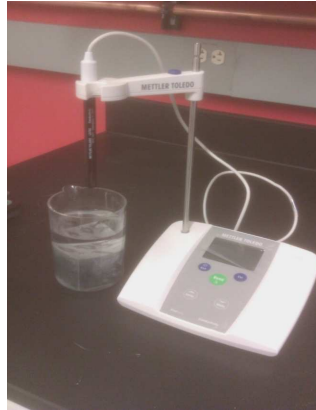
Figure 3.6: Conductivity Meter with the Sample

3.7 Reaction Product Analysis

3.7.1   ATR – FTIR Spectroscopy

Attenuated total reflectance – Fourier transform infrared spectroscopy (ATR-FTIR) allows the determination of transmission spectra without destructive sample preparation. Spectra are obtained from the absorption or transmittance of a wave which is transmitted through an internal reflection element (IRE) of high refractive index and penetrates a short distance into the sample, in contact with

the IRE. The IRE used is diamond, selected because of its resistance to high pH and abrasion from sample removal and cleaning. A picture of the ATR attachment along with a schematic diagram of the beam path through the apparatus is shown in Figure 3.7.
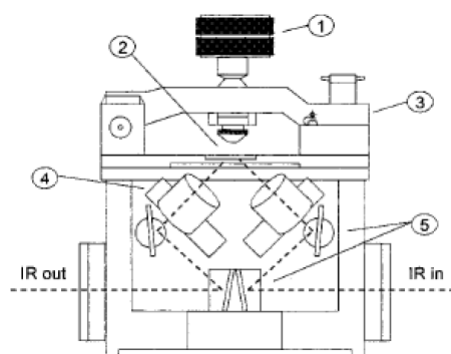
(a)   (b)

Figure 3.7: (a). ATR attachment, (b). Schematic diagram showing the beam path through the ATR (1) torque head screw with limiter screw; (2) ATR crystal, (3) clamp bridge, (4) lens barrel, (5) mirrors. [Tuchbreiter et al. 2001]

4. REACTION KINETICS IN SODIUM SILICATE SOLUTION (WATER GLASS) ACTIVATED SLAG AND FLY ASH-SLAG BINDERS EVALUATED USING ISOTHERMAL CALORIMETRY

The kinetics of alkali activation is highly dependent on the chemical composition and the activator concentration. In this chapter, the influence of binder composition (amounts of fly ash and slag in the blend), alkali concentration, as expressed using the ratios of Na_2O-to-binder (n) and Silicate modulus, expressed as the ratio of SiO_2-to-Na_2O (M_s), on the reaction kinetics of sodium silicate solution (waterglass) activated slag and fly ash-slag binder systems are examined. Optimal binder composition and n values are determined from the setting time data which are then used to determine the reaction kinetics using isothermal calorimetry experiments. The influence of temperature on the reaction kinetics of fly ash-slag blends are discussed based on the hydration parameters. Finally, kinetic modeling is used to quantify the distinction in the reaction kinetics using different modeling methods and is compared to that of ordinary cement hydration.

4.1 Selection of Optimal Source Material and Activator Parameters

4.1.1   Influence of binder composition on the setting time

As described before, one of the major intentions of this study was to develop activated fly ash binders that can attain acceptable compressive strengths under normal moist curing conditions. Slag is used as the major constituent to achieve acceptable early age properties since it is well known that fly ash activation requires heat. In this study, the initial setting time is used as a basis for identifying

36

the acceptable binder compositions and n values to be used for extensive compressive strength (details given in Chapter 5) and calorimetry studies.

Table 4.1: Initial and the final set values

Binder Composition	n	M_s	Initial Set (mins)	Final Set (mins)
100% Slag	0.03	1	541	946
	0.03	2	53	156
	0.05	1	337	437
	0.05	2	33	72
	0.075	1	110	270
	0.075	2	27	62
50% Fly ash–50% Slag	0.05	1	-	
	0.05	2	64	169
	0.075	1	497	640
	0.075	2	58	114
70% Fly ash–30% Slag	0.075	1	-	
	0.1	1	627	1032
	0.1	2	133	231
70% Fly ash–20% Slag-10% Metakaolin	0.075	1	-	
	0.1	1	639	1042
	0.1	2	172	242
80% Fly ash–10% Slag-10% Metakaolin	0.075	1	-	
	0.1	1	-	
	0.1	2	375	510
85% Flyash–15% Slag	0.075	1	-	
	0.1	1	-	
	0.1	2	347	465

Initial and final setting times of alkali activated fly ash, slag, or blended systems depend mainly on the binder composition, activator type and its concentration. Table 4.1 shows the initial and the final setting times of a number of unary, binary and ternary component alkali activated systems containing slag, fly ash, and metakaolin. Alkali activated mixtures with slag alone as the starting material

reaches its initial setting time faster than the fly ash rich mixes; the mixtures that use fly ash alone as the starting material do not reach their initial set in 12 hours for the activator characteristics used in this research work as shown in Figure 4.1
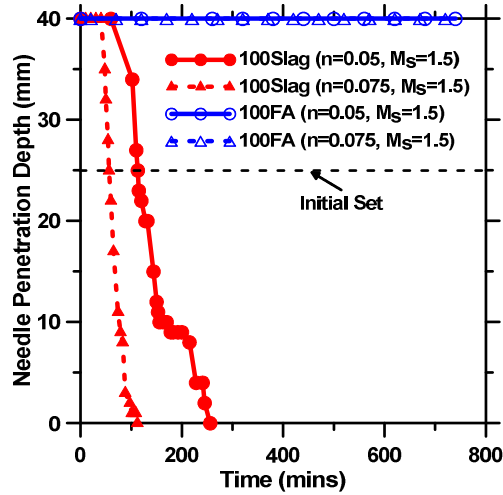
Figure 4.1: Initial and final setting times of slag and fly ash activated pastes
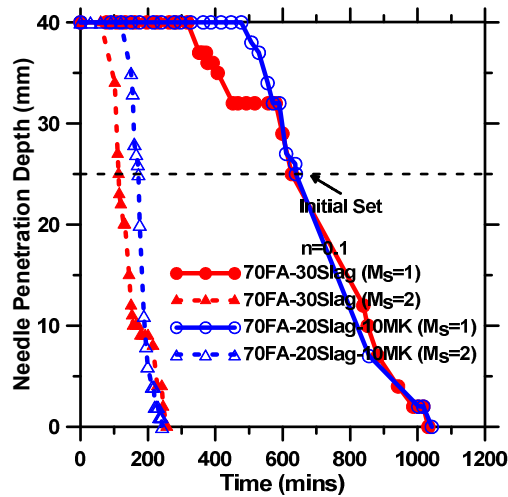
Figure 4.2: Comparison of the initial and the final setting times of fly ash rich blends with and without the addition of metakaolin.

It has been reported that activated mixtures with fly ash alone as the source material require heat for activation [Paloma et al. 1999, Van Jaarsveld et al. 1997, Vargas et al. 2011]. The addition of small amounts of metakaolin to the system does not result in any significant changes in the setting times as shown in Fig 4.2.

4.1.2   Influence of activator parameters (n and M_s) on the setting time of waterglass activated systems

From Table 4.1 it can be inferred that higher the n and M_s values, the faster the initial and the final setting times. For the same n value, a change in activator M_s from 1 to 2 results in a much larger impact on setting times, i.e. the apparent effect of SiO_2 on setting behaviour is more pronounced than that of Na_2O. In other words, the mixtures with lower n and higher M_s values set faster than the mixtures with higher n and lower M_s values. This is because a higher concentration of $[SiO_4]^{4-}$ increases the reaction rate [Chang et al. 2003]. This trend is observed irrespective of binder composition and the same is shown in Figure 4.3 for activated slag with n values of 0.05 and 0.075 and M_s of 1, 1.5 & 2. Reducing the amount of slag in the mixtures necessitates a higher alkalinity. For the fly ash-slag blended mixtures, the 50% fly ash – 50% slag mixture proportioned with an n value of 0.05 and Ms of 1 does not reach its initial set in 12 hours. A higher n value of 0.075 is required to reach initial set in less than 12 hours as shown in the Figures 4.4 (a) and (b). The 70% fly ash – 30% slag and 85% fly ash – 15% slag mixtures also do not reach their initial set when an n

value of 0.075 and Ms of 1 is used. An n value of 0.1 is required in these cases as shown in Figures 4.5 (a) and (b); this illustrates the influence of a Ca bearing starting material on the early age response of alkali activated systems.
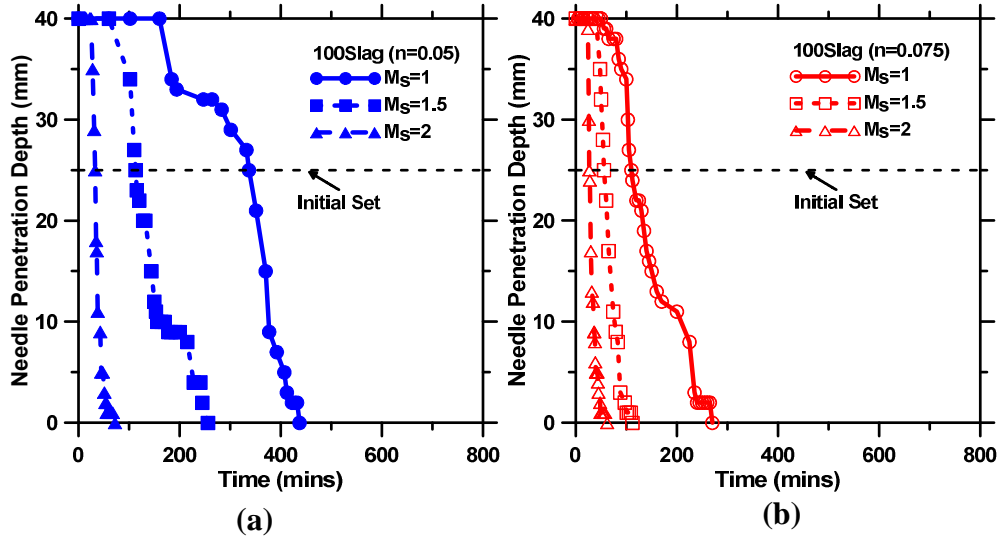
Figure 4.3: Comparison of setting times of 100% Slag with different n values
(a) n=0.05 (b) n=0.075
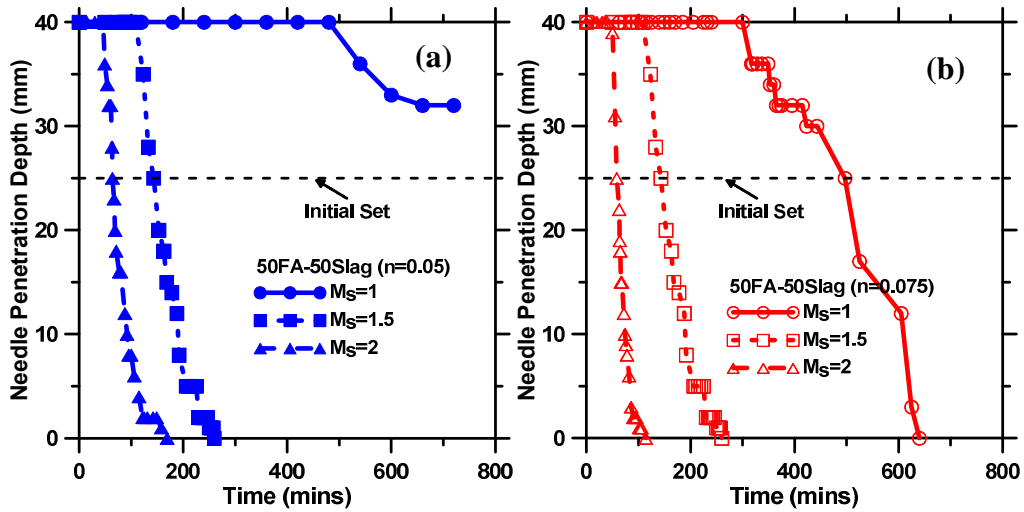
Figure 4.4: Comparison of setting times of 50% fly ash–50% slag mixture
proportioned with an n value of (a) 0.05 and (b) 0.075

40
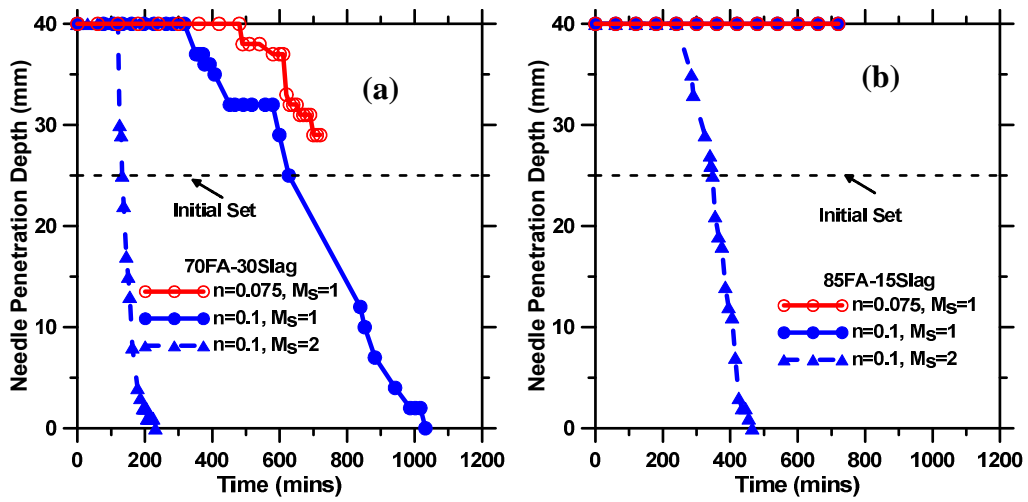
Figure 4.5: Comparison of setting times of fly ash rich blends proportioned using different n values (a) 70% fly ash-30% slag and (b) 85% fly ash-15% slag.
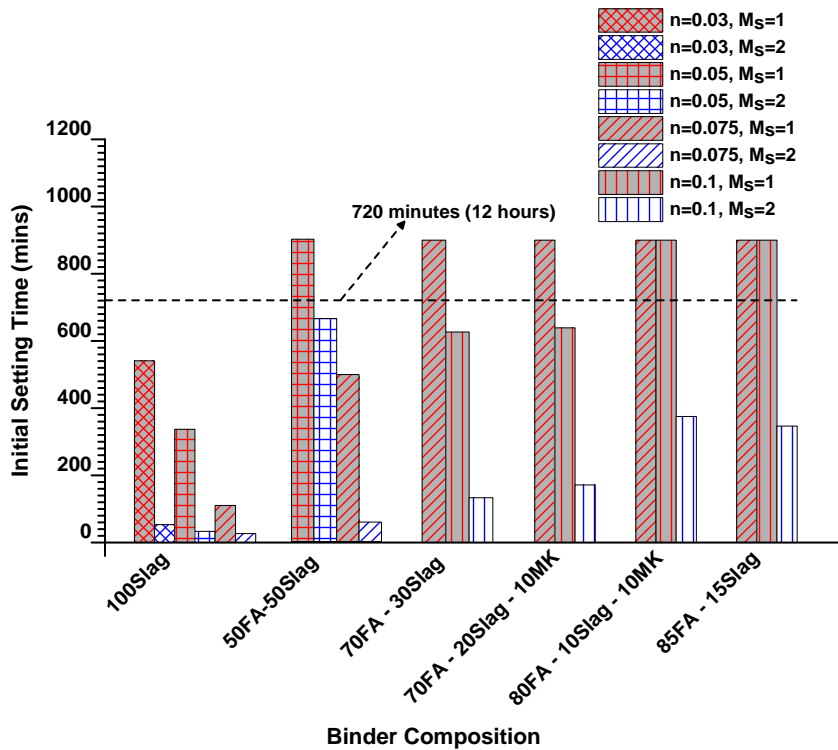
Figure 4.6: Selection of binder composition and n value based on the setting time. Mixes that reach initial set in 12 hours are selected

By extensively performing the setting time experiments the influence of binder composition and the n and M_s values on the early age behavior of the slag and fly ash-slag blends are determined. Mixtures that set in a reasonable time (12 hours) are selected for further experiments and are summarized in Figure 4.6. The minimum n values at which desirable initial setting is obtained for those mixtures are shown in Table 4.2. For further studies on calorimetric and mechanical response of these materials, these n values are used along with both lower and higher M_s values (1 and 2).

Table 4.2: Minimum n values for which the mix reaches its initial set in 12 hrs

Binder composition	n value
100% Slag	0.03[A]
50%FA – 50%Slag	0.075
70%FA – 30%Slag	0.1
70%FA – 20%Slag – 10%MK	0.1

[A] The n value used for calorimetric experiments in this case is 0.05 because this has been determined to be an optimal value [Wang et al. 1994]. The details are clarified in Chapter 5

4.2 Isothermal Calorimetric Studies on Slag and Fly ash-Slag Blends

4.2.1 Comparison of calorimetric signatures of activated slag and cement

Figure 4.7 shows the heat evolution curves for waterglass activated slag pastes proportioned using an n value of 0.05 and M_s values of 1 and 2. The calorimetric response exhibits two peaks.
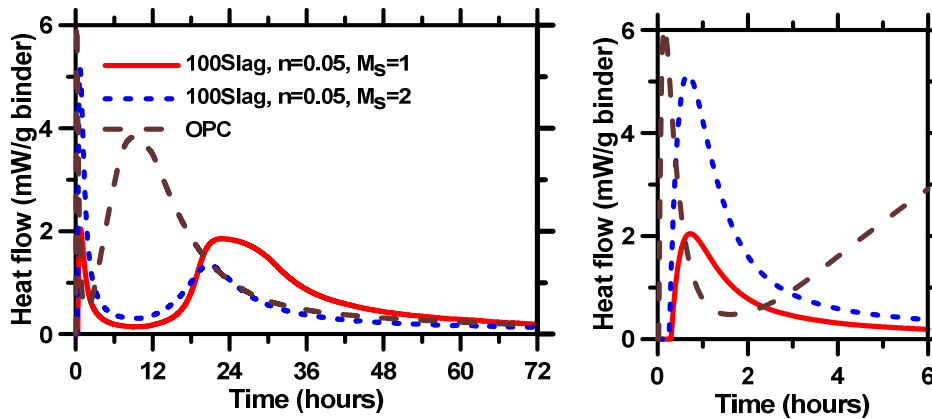
Figure 4.7: Comparison of calorimetric response of waterglass activated slag with ordinary Portland cement hydration. The right graph magnifies the initial 12 hours of heat evolution curves for the same sample.

The very early narrow peak within the first few hours of mixing corresponds to the particle wetting and the dissolution of slag particles [Shi and Day 1995, Ravikumar and Neithalath 2012]. The dormant period that follows this peak is followed by an acceleration peak that is smaller in magnitude. The shape of the heat release curve is similar to that of OPC hydration even though the significant features are different with respect to their magnitudes and their occurrences in the time scale. The heat release curve for an OPC paste at a water-to-cement ratio (w/c) of 0.50 is also shown in Figure 4.7 to facilitate comparison. The induction period in waterglass activated slag paste is found to be considerably longer than that of the OPC paste, in line with observations reported previously [Ravikumar and Neithalath 2012]. This is because of the time required for the ionic species in solution to reach a critical concentration to form reaction products. The waterglass activated pastes also have a much smaller acceleration peak, bringing into view the contrast with OPC as far as reaction kinetics is concerned. Decrease in Ms (or

43

increase in alkalinity) resulted in broader acceleration peak for the waterglass activated slag pastes suggesting improved activation.

4.2.2 *Calorimetric signatures of fly ash rich blended pastes activated using waterglass*

Figures 4.8 (a) and (b) show the heat evolution as a function of time for waterglass activated fly ash-slag pastes proportioned using activator M_s of 1 and 2 for n-values of 0.075 for the 50%fly ash-50%slag blend and 0.10 for the 70%fly ash-30%slag blend. Instead of the two-peak system observed for the OPC and activated slag pastes, the waterglass activated fly ash-slag systems show only one large peak that is generally observed within the first 2-3 hours. The only exception is the 50%fly ash-50%slag blend with M_s of 1 (higher alkalinity) that demonstrates a broader, low intensity peak after 20 hours. The general single-peak trend in these mixtures is because of the fact that the dissolution of some of the initial materials happen early along with some gelation to form reaction products but no additional reaction products of exothermic kinetics are formed until much later (beyond the time that calorimetric experiments are conducted). It is anticipated that when the later reactions take place, the heat release rate is in all probability slow and low. In both the slag and fly ash-slag blended systems, the initial dissolution peaks are narrower and steeper for pastes with higher M_s. This is due to the acceleration in the initial reaction due to high amounts of $[SiO_4]^{4-}$ ions. This corresponds to the faster setting of these mixes as seen in setting time

data. The appearance of the low intensity acceleration peak in the lower M_s paste can be attributed to the C-S-H gel formation in a diluted Ca containing system (only 50% of slag) under the influence of higher activator alkalinity. For the 70% fly ash-30% slag blend, the Ca ion concentration in the system is so low that a meaningful acceleration peak is absent. In this case, as well as the case for the 50%fly ash-50%slag blend with a higher M_s value, the reaction products are formed by initial gelation, and further progress is diffusion controlled that results in little changes in the calorimetric signatures.
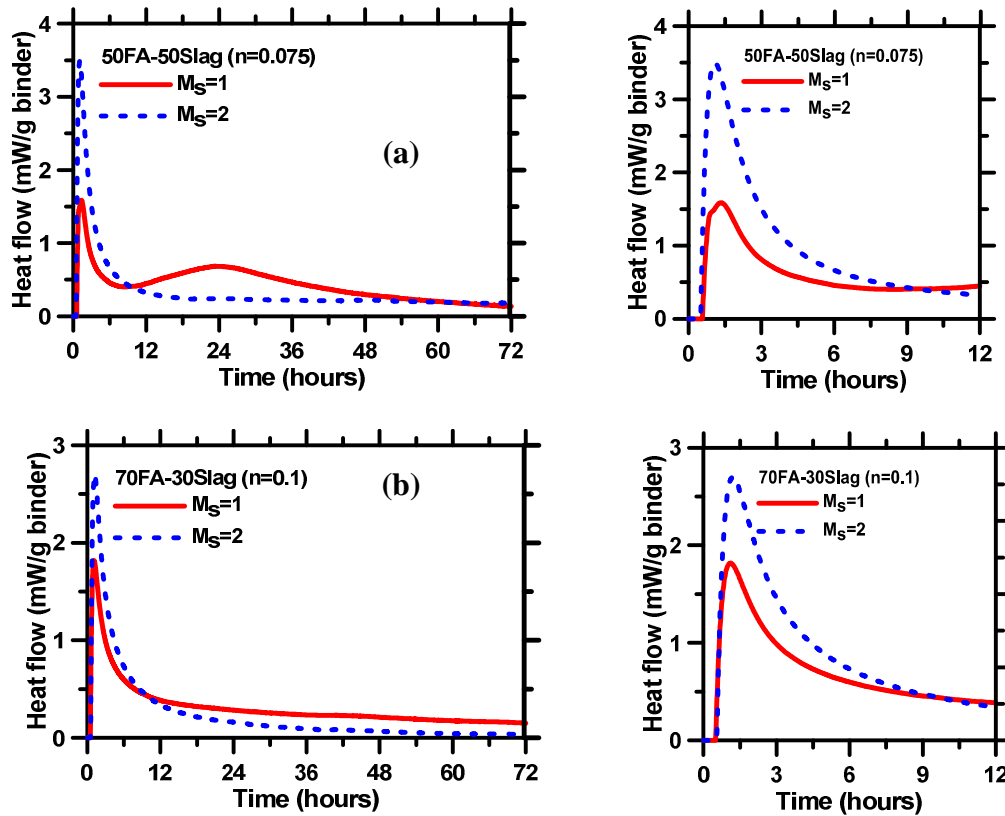
Figure 4.8: Calorimetric response of fly ash rich blends (a) 50% Fly ash – 50% Slag and (b) 70% Fly ash – 30% Slag for 72 hours. The right graph magnifies the initial 12 hours of heat evolution curves for the same sample.

4.3 Cumulative Heat Release and its use for Kinetic Modeling

The cumulative heat released Q(t), obtained by integrating the heat flow curves, is shown in the Figure 4.9 for the waterglass activated slag mixes maintained at $25^{o}C$.
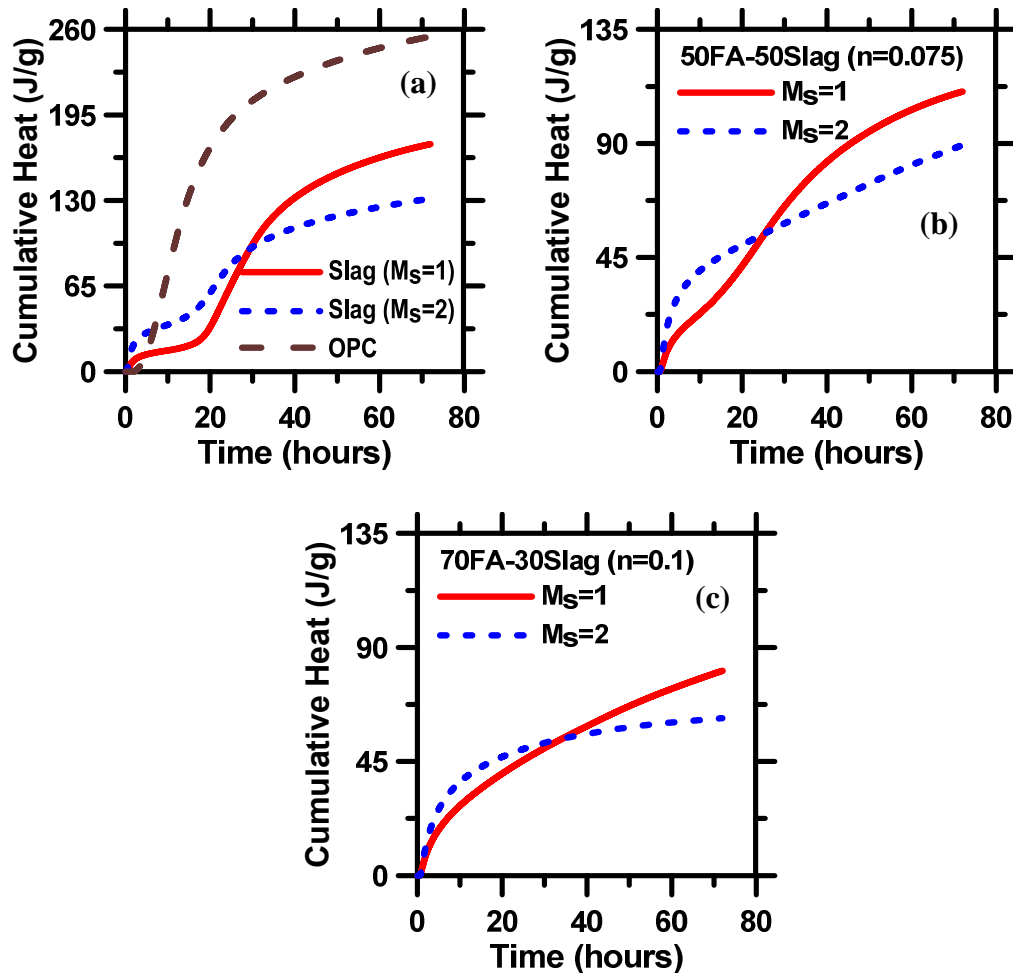
Figure 4.9: The cumulative heat release of (a) 100% slag (n=0.05), (b) 50% Fly ash – 50% Slag and (c) 70% Fly ash – 30% Slag for 72 hours.

The initial ascent depicts the heat release contribution due to dissolution and the subsequent climb depicts the heat release contribution due to the acceleration peak. The induction period is represented by the relatively flatter regions in the

46

cumulative heat release curve between the initial dissolution rise and the latter acceleration rise. Cumulative heat release is initially high for mixes with higher M_s due to faster reaction facilitated by the high amount of SiO_4 ions. However the total cumulative heat release after 72 hours is high for mixtures with a higher alkalinity (lower M_s and/or higher n). Furthermore, the cumulative heat release values of waterglass activated slag systems are lesser than that of OPC after 72 hours and can be inferred from the Figure 4.9 (a). The heat released for the waterglass activated fly ash-slag blends is contributed by a single dissolution gelation peak represented by a single curve behaviour in the cumulative heat release except in the case of 50% fly ash and 50% slag with lower silicate modulus (M_s=1) where a small bulk hydration peak appears.

4.4 Influence of Temperature on Calorimetric Response

4.4.1 Comparison of the influence of temperature on the hydration of activated slag and fly ash rich blends

The influence of temperature on the reaction kinetics of slag, fly ash, and their blends is elucidated in this section using the calorimetry tests conducted on waterglass activated slag and fly ash-slag blended pastes, and NaOH activated fly ash pastes at 25°C, 35°C, and 40°C . The temperature-linked heat release curves for a typical OPC paste is also shown for comparison. For the slag and fly ash-slag blends, pastes with M_s of 2.0 were selected for studies on the influence of temperature. This was because these pastes demonstrated a weaker or non-

47

existent acceleration peak at 25°C, and thus the effects of increasing temperature are more pronounced.
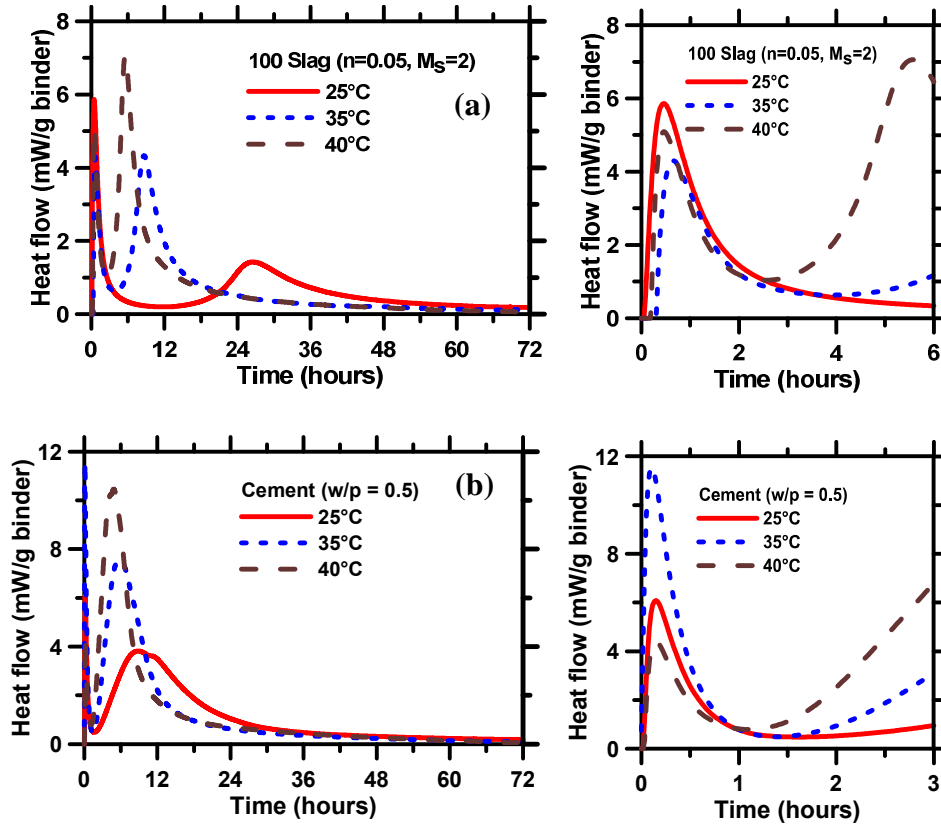
Figure 4.10: Influence of temperature on the calorimetric response, the left graphs represent the heat evolution rate of (a) 100% slag (n-0.05, M_s=2) and (b) OPC (w/p=0.5 for 72 hours. The right graph magnifies the initial 12 hours of heat evolution curves for the same sample.

Figure 4.10 (a) shows the heat release response of activated slag pastes at the three chosen temperatures while Figure 4.10(b) shows the response of an OPC paste for comparison since it was shown earlier that the response of activated slag is similar to that of OPC at ambient temperatures. For the waterglass activated slag pastes, an increase in temperature from 25°C to 35°C results in significant changes in the calorimetric response, especially with respect to the temporal

48

location of the acceleration peak. Such a drastic change is not noticed for the OPC paste, even though the peak intensities change significantly in both the cases. A comparison between Figures 4.10(a) and (b) reveals the influence of temperature on hydration of both slag and OPC.

Figures 4.11 (a) and (b) depict the calorimetric response of 8M NaOH activated fly ash and waterglass activated 50% fly ash-50% slag blend (n=0.075, Ms=2) pastes respectively. Figure 4.11 (a) shows that an increase in temperature has a profound effect on the heat release rates for the fly ash rich blends. However, the acceleration peak that was conspicuous in activated slag systems and which made an appearance in the ambient temperature response of the 50% fly ash-50% slag blend at an M_s of 1 is absent in this case. The dissolution of the glassy phases of fly ash and their gelation is taking place simultaneously as indicated by the single peak response. The significant increase in peak intensity at higher temperatures indicates an increased amount of reaction products during early stages. This result in the further diffusion controlled reactions being slowed down, consequently influencing the rate of property development in such systems. From Figure 4.12 (a) it can be seen that the two-curve behavior observed for the activated slag paste at 25°C disappears at higher temperatures (35°C and 40°C) since the induction period is shortened by the acceleration in reaction rate due to the increased temperature. Table 4.3 shows that the increase in temperature increases the cumulative heat release after 72 hours in slag paste and also the OPC paste. The cumulative heat release values are of waterglass activated slag pastes are lower

than that of the OPC paste. The maximum cumulative heat release (at 40°C) after 72 hours for waterglass activated slag paste is found to be 190 J/g when compared to that of OPC paste where it is 310 J/g (See Table 4.3).

Figure 4.11(a) shows the influence of temperature on the calorimetric response of 100% fly ash activated with 8M NaOH. At room temperature, the calorimetric responses of this paste and that of the 50% fly ash-50% slag blend are very similar. However, note the Y-axes scales which are very different in both the cases, suggesting the extent of exothermicity of the reactions. When the reaction temperature is increased, while there is no subsequent exothermic processes after the initial dissolution-gelation peak in the waterglass activated fly ash-slag blend, a distinct secondary exothermic process is observed for the NaOH activated fly ash paste. The process of dissolution of fly ash in a highly alkaline solution entails the breakdown of the covalent Si-O-Si and Al-O-Al bonds in the glassy phase of fly ash and the release of these ions into the pore solution. At room temperatures, structure formation does not happen because of the high activation energy barrier. At elevated temperatures, polycondensation happens, which is exothermal, leading to the secondary peaks in the isothermal calorimetry response. This step culminates in the formation of reaction products (N-A-S-H gel in this case) with a poorly ordered structure but a high mechanical strength [Paloma et al 1999]. The cumulative heat releases shown in Table 4.3, 105 J/g and 146 J/g for the pastes maintained at 35°C and 40°C after 72 hours, compared to 12.5 J/g at 25°C demonstrates this effect. A 10°C in the reaction temperature results in an almost

10-fold increase in the cumulative heat released, showing the effect of temperature on the activation of NaOH activated fly ash pastes. It can also be inferred from Figure 4.12 (b) that the influence of temperature for fly ash-slag blends is more pronounced and hence the difference in the cumulative heat flow curves are much larger for fly ash-slag blends when compared to slag and OPC systems. Similar effect can be seen in Table 4.3 with higher difference in cumulative heat release for fly-ash rich blends at higher temperatures.
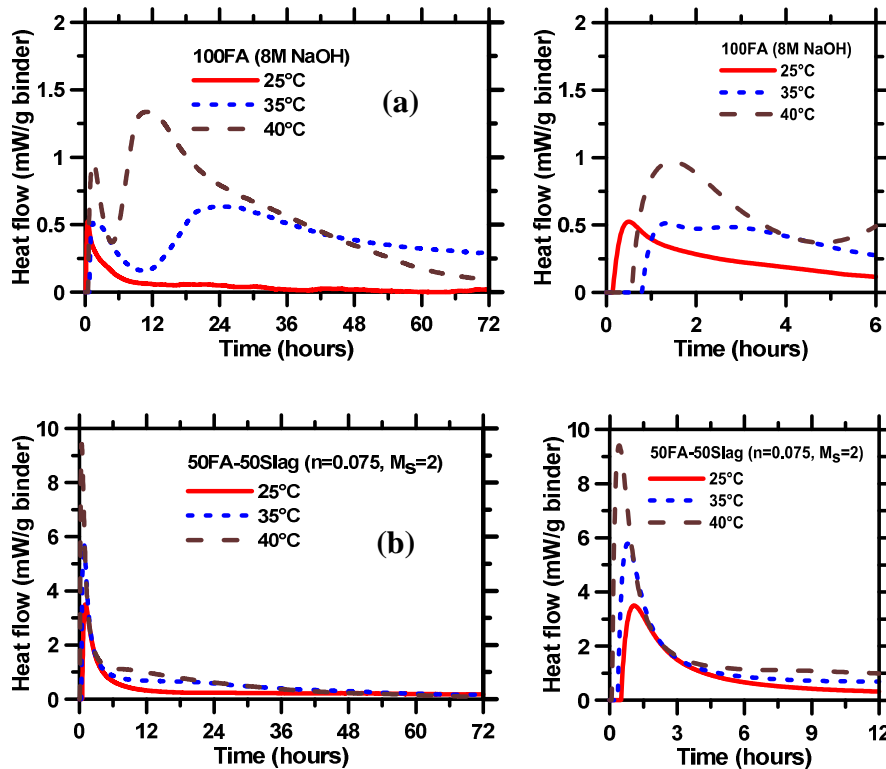
Figure 4.11: Influence of temperature on the calorimetric response of, (a) 100% fly ash (8M NaOH). and (b) 50% fly ash-50% slag blend, The left graph represents the heat evolution rate for 72 hours. The right graph represents the heat evolution rate at early ages (until 12 hours)
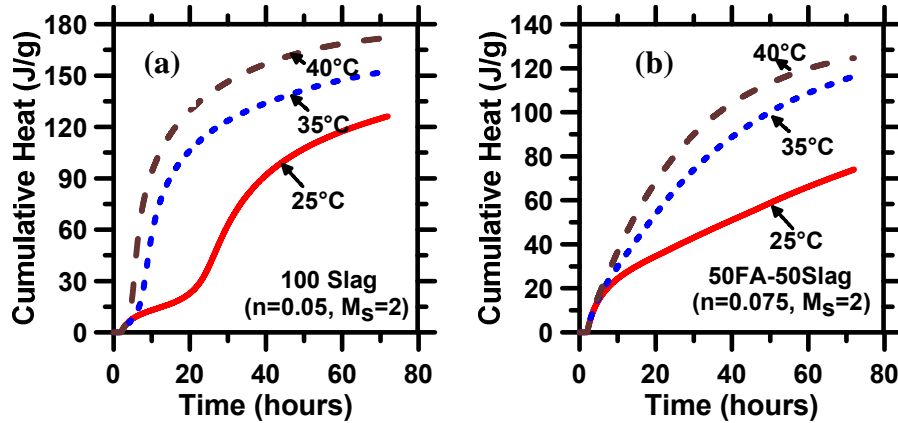
Figure 4.12: Influence of temperature on the cumulative heat release of (a) 100%
Slag (n=0.05), (b) 50% FA – 50% Slag (n=0.075)

Table 4.3: Heat curve analysis

Binders	n	M_s	T (°C)	Peak Value (mW/g)		Time of appearance of peaks (hrs)		Cumulative heat released after 72 hours (J/g)
				I	II	I	II	
Slag (100%)	0.05	2	25	5.86	1.43	0.45	26.28	150.1
			35	4.3	4.33	0.65	8.62	169.19
			40	5.09	7.06	0.45	5.57	190.58
Fly ash-Slag (50%-50%)	0.05	2	25	3.78	-	0.55	-	60.49
			35	9.65	-	0.22	-	117.36
			40	3.98	0.704	0.65	25.47	120.39
	0.075	2	25	3.5	-	1.07	-	89.36
			35	5.78	-	0.78	-	140.68
			40	9.42	-	0.42	-	161.56
Fly ash-Slag (70%-30%)	0.075	2	25	3.21	-	0.63	-	67.88
			35	5.7	-	0.63	-	90.23
			40	10.1	-	0.25	-	96.66
	0.1	2	25	2.69	-	1.15	-	62.07
			35	4.71	-	0.78	-	93.08
			40	12.3	-	0.2	-	113.83
Fly ash (100%)	8M NaOH		25	0.525	-	0.5	-	12.51
			35	0.514	0.635	1.33	24.77	104.6
			40	0.97	1.34	1.45	10.57	145.74
OPC	NA		25	6.09	3.82	0.15	8.67	266.64
			35	11.5	7.47	0.1	5.43	287.62
			40	4.41	10.5	0.15	4.78	309.99

4.5 Kinetic Modeling

4.5.1   *Comparison of exponential and Knudsen models based on the cumulative*

   heat release

The maximum cumulative heat released Q_{max} is determined by two different

methods in order to identify the effect of different hydration parameters on the

reaction kinetics.

In Method I the values of Q_{max} can be obtained by fitting an exponential model to

the cumulative heat flow curve [Neithalath 2008] given by the following equation.

$$Q(t) = Q_{max}e^{\left(-\left[\frac{\tau}{t}\right]^{\beta}\right)} \qquad \textbf{4.1}$$

Q_{max} is the maximum heat that could be released because of the reaction. τ is the

hydration time parameter and β is the shape parameter.

In Method II the total heat evolution of cement with time is described by the

semi-empirical equation (Knudsen 1980, Roy and Idorn 1982, 1985, Shi et al.

1991a, Zhou et al. 1993, Fernandez-Jimenez and Puertas 1997b):

$$Q(t) = Q_{max} \cdot \left[\frac{K.(t-t_o)}{1+K.(t-t_o)}\right] \qquad \textbf{4.2}$$

Where $Q(t)$ = total heat evolution at time t (kJ/kg); Q_{max} = total heat evolution at

t=∞ (kJ/kg); K is a constant parameter which is equal to the reciprocal of t_{50},

where t_{50} is the time to achieve 50% of Q_{max}; t = actual hydration time at

temperature T (hours); t_o = time parameter. In order to maintain uniformity, time

to reach isothermal conditions is taken as 2 hours after the start of the test for

53

calculating Q_{max} using both these methods, i.e the heat released in the first two hours are not considered for the Q_{max} calculation.

Activation energy which is the minimum energy required to start a chemical reaction is defined by the Arrhenius law using the equation 4.3

$$K(T) = A.e^{\left[\frac{-E_a}{RT}\right]} \qquad \textbf{4.3}$$

Where K(T) is the rate constant determined at different temperatures. A is a pre-exponential factor that does not change much with temperature. E_a is the activation energy, T is the temperature (in K) and R is the universal gas constant (in J/K/mol) .The slope of the plot ln K(T) vs 1/T gives the slope $-E_a/R$ from which activation energy can be determined.

4.5.2 *Influence of binder composition and temperature on the hydration parameters*

The hydration parameters are influenced to a large extent by the binder composition. Table 4.4 gives the predicted Q_{max} values based on the fit of Q (t) and t plots using Method I and Method II for activated slag paste and ordinary Portland cement paste. Q_{max} increases with an increase in temperature for same binder composition and alkali concentration. τ and t_o values corresponding to the hydration time decreases with the increase in the temperature since the induction period and the time to reach the starting point of the acceleration period in both slag and cement decreases with increase in temperature.

Table 4.4: Q_{max} values based on Method I and II for activated slag and OPC

Binders	T (°C)	Method I $Q_{max}e^{\left(-\left[\frac{\tau}{t}\right]^{\beta}\right)}$			Method II $Q_{max}\cdot\left[\frac{K.(t-t_o)}{1+K.(t-t_o)}\right]$			E_a (KJ/mol)
		Q_{max} (J/g)	τ (hrs)	β	Q_{max} (J/g)	t_o (hrs)	K (hrs^{-1})	
Slag (n=0.05, M_s=2)	25	162.2	29.1	1.59	175.7	6.10	0.030	56.7
	35	159.5	10.6	1.40	192.7	2.42	0.060	
	40	183.1	7.8	1.17	201.1	1.71	0.091	
OPC	25	274.4	11.8	1.35	334.6	2.60	0.051	46.8
	35	276.1	7.10	1.36	310.3	1.65	0.106	
	40	314.1	6.1	1.12	335.6	1.33	0.122	

t_o values are always lesser than that of τ for the same mix at the specified temperature; therefore the predicted Q_{max} determined using Knudsen method (Method II) is found to be higher than the Q_{max} values determined using the exponential method (Method I). The value of β decreases with the increase in the temperature. This can be related to the decrease in the slope of the cumulative heat release curves with temperature.

The t_0 value determined using Knudsen method gives a better estimate of the second peak corresponding to the end of induction period (start of the acceleration peak) in the case of cement paste, similar to that reported by other researchers (Knudsen 1980, Roy and Idorn 1982, Fernandez-Jimenez 1997b). However the τ value determined using the exponential method gives a superior assessment of the second peak in the case of activated slag pastes and can be related to the time to the end of acceleration. This can be attributed to the distinct changes in the shape of the curve (from two curves to a single curve) with increasing temperature in the

case of slag pastes. Hence the exponential method with the shape parameter β gives a better indication of the reaction kinetics in this case. The parameter K determined using the fits increases with an increase in the temperature in the case of slag and cement pastes and it is found to be equal to the reciprocal of the time to achieve 50% of Q_{max}. Hence this constant parameter can be considered as a rate determining parameter in the case of slag and cement. These rate constant values can be used in determining the apparent activation energy (E_a) using Arrhenius law using equation 4.3 and are shown in Table 4.4. The E_a value for activated slag are higher (56.7 KJ/mol) than that of cement (46.8 KJ/mol). This shows even with the introduction of alkalis into the system the alkali activated slag requires higher activation energy to initiate the reaction.

Table 4.5 gives the predicted Q_{max} values based on the fit of Q(t) vs. t plots using Method I and Method II for fly ash rich blends. Q_{max} values increases with an increase in the temperature for the same binder composition and alkali concentration. However the difference in Q_{max} values at higher temperatures (35°C and 40°C) are significantly higher in the case of fly ash rich blends where the reaction rate at higher temperature increases in comparison to the very low or non-existent reactivity at ambient temperature (note the very low Q_{max} values). t_o values are always lesser than that of τ for the same mix at the specified temperature similar to activated slag and cement pastes; however the predicted Q_{max} determined using Knudsen method (Method II) is found to be lower than the Q_{max} values determined using the exponential method (Method I) in most cases.

56

Table 4.5: Q_{max} values based on Method I and II for fly ash rich blends

Binders	n	M_s	T (°C)	Method I $Q_{max}e^{\left(-\left[\frac{\tau}{t}\right]^{\beta}\right)}$			Method II $Q_{max}\cdot\left[\dfrac{K.(t-t_o)}{1+K.(t-t_o)}\right]$		
				Q_{max} (J/g)	τ (hrs)	β	Q_{max} (J/g)	t_o (hrs)	K (hrs^{-1})
Fly ash-Slag Blends (50%-50%)	0.5	2	25	51.7	16.20	0.70	54.2	0.50	0.032
			35	195.7	58.00	0.70	166.7	2.01	0.012
			40	270.9	64.19	0.57	250.1	2.46	0.011
	0.075	2	25	86.2	14.41	0.74	82.0	1.53	0.048
			35	165.0	21.47	0.79	143.6	2.62	0.042
			40	200.4	21.75	0.66	182.5	1.77	0.033
Fly ash-Slag Blends (70%-30%)	0.075	2	25	80.5	17.17	0.52	62.7	0.79	0.054
			35	85.1	13.85	0.60	72.7	0.98	0.058
			40	93.7	13.55	0.62	81.4	1.05	0.058
	0.1	2	25	63.9	9.36	0.69	59.0	1.02	0.078
			35	105.6	16.45	0.56	85.8	0.91	0.053
			40	112.1	17.01	0.58	93.0	1.05	0.049
Fly ash (100%)	8M NaOH		25	15.6	17.34	0.59	13.0	1.07	0.047
			35	185.0	19.00	0.95	164.0	3.01	0.020
			40	202.0	23.03	0.96	266.0	3.36	0.019

The reaction mechanism of fly ash rich blends should be better understood in order to estimate the hydration parameters, however the parameters do not seem to follow any trend in these cases. It is found that the constant parameter K decreases with an increase in temperature from 25°C to 35°C due to the vast difference in the Q_{max} values in this case. This shows that an increase in 10°C allows the material to overcome its activation energy barrier and react to form binding compounds. This is an important observation that has implications in deciding the optimal curing parameters for desired reactivity and mechanical properties. Since the values of K decreases with temperature it cannot be

considered as a rate determining parameter in the case of fly ash rich blends and hence it cannot be used in determining the apparent activation energy (E_a). However, with another temperature, perhaps higher than the 35^oC, used for calorimetric experiments, might result in the same approach being capable of extracting the activation energies.

4.5.3   *Influence of two-curve analysis in activated slag systems*

Since waterglass activated slag paste show a two part calorimetric signature, with an initial peak corresponding to the dissolution of slag particles and the second bulk peak corresponding to precipitation of the reaction products, it is expected that a two-part equation would be ideal to fit the cumulative heat release response. This helps in separating out the influence of the activator on the dissolution and precipitation reactions individually. Figure 4.13 shows a representative fit of the hydration heat curve using the two-part equation explained above. The second curve starts from a point in the induction period determined by drawing tangents at the ascending portion of the second curve and extending the tangent to meet the x-axis. The $Q(t)$ value corresponding to this point on the x-axis is considered as the starting point for the second curve.

The values of τ, β, t_o and K reported in Table 4.6 corresponds only to the second part of the curve. It should be noted that since the mixing of the paste is done outside the calorimeter, a significant part of the first phase is lost and hence the Q_{max1} value might not be very accurate.

Table 4.6: Q_{max} values based on the 2 curve fit approach for slag mixes

T (°C)	Method I $Q_{max}e^{\left(-\left[\frac{\tau}{t}\right]^{\beta}\right)}$				Method II $Q_{max} \cdot \left[\frac{K.(t-t_o)}{1+K.(t-t_o)}\right]$			
	Q_1 (J/g)	Q_2 (J/g)	τ (hrs)	β	Q_1 (J/g)	Q_2 (J/g)	t_o (hrs)	K (hrs^{-1})
25	42.5	141.1	27.4	2.19	39.9	182.0	17.6	0.02
35	25.8	159.4	10.64	1.41	24.2	169.8	5.81	0.12
40	12.2	183.9	7.76	1.15	11.5	191.4	3.16	0.13
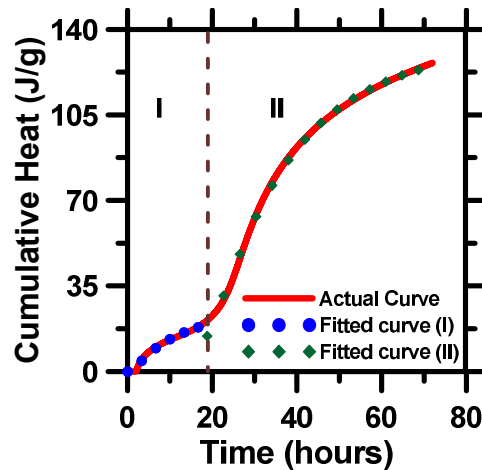
Figure 4.13: Two-curve fitting for the cumulative heat release of slag (n=0.05, Ms=2) (experiments done at 25°C)

The Q_{max2} values (which are equivalent to the Q_{max} values shown in Table 4.4 for the corresponding temperatures) are lower when predicted using the two-curve fitting method. The constant parameter K determined using Knudsen equation increases with temperature. However the difference in the K values are large (from 25°C to 35°C) for to calculate the apparent activation energy. While this is

a useful method to predict the accurate heats of hydration, the vast difference in the rate determining parameter K with temperature seems to somewhat diminish the applicability of this methodology.

4.6 Summary

The influence of binder composition, activator concentration and temperature on the reaction kinetics of sodium silicate activated slag and fly ash-slag blends are discussed in this chapter. Optimal binder composition and n values are selected based on the initial setting time. The influence of binder composition, activator parameters (n and M_s) and temperature on the isothermal calorimetric response was reported. The waterglass activated slag systems showed a calorimetric response similar to those of OPC pastes with a marked induction period. Kinetic modeling was used to quantify the differences in reaction kinetics using two different modeling methods. The constant K determined using the Knudsen method is considered as a rate determining parameter in the case of activated slag and cement (when the difference in the Q_{max} values are not very large with an increase in temperature) and can be used in calculating the apparent activation energy. However it cannot be considered as a rate determining parameter in the case of fly ash rich blends since the difference in the Q_{max} values are very large with increases in temperature (especially from 25°C to 35°C). The K values allow for the determination of the optimal curing parameters for desired reactivity and mechanical properties. The activation energy determined using rate constant

values (based on Arrhenius law) are found to be higher for activated slag (56.7 KJ/mol) when compared to that of cement (46.8 KJ/mol).

5. INFLUENCE OF ACTIVATOR PARAMETERS ON THE STRENGTH AND REACTION PRODUCTS IN ALKALI SILICATE ACTIVATED SLAG AND FLY ASH – SLAG BLENDS

In this chapter, the influence of curing duration, binder composition and activator characteristics on the compressive strength development of, and the reaction product formation in sodium silicate solution activated slag and fly ash-slag binder systems are examined. ATR-FTIR analysis was used to characterize the reaction product. The strength losses in highly alkaline mixtures are explained through quantification of leaching by performing electrical conductivity of the solutions in which the specimens were submerged in. The influence of curing conditions (open (dry), open (moist) and closed) on the compressive strength development of heat-cured fly ash mixtures and its ATR-FTIR analysis are also reported.

5.1 Compressive Strength of Slag and Fly ash-Slag Binders

5.1.1   Influence of curing duration, binder composition and activator

characteristics on the compressive strength of slag mortars

Compressive strengths of the waterglass activated slag mortar specimens that were moist-cured were determined at ages of 3, 14, and 28 days and are shown in Figures 5.1 (a), (b), and (c) respectively as a function of the n and M_s values. The mortars were prepared as explained in Chapter 3. Three different n values (0.03, 0.05, and 0.075), and three M_s values (1.0, 1.5, and 2) are used. The compressive strength response of slag mortars is used here as a basis to which the properties of

the fly ash-slag blend can be compared to. The compressive strength of activated slag mortars increase with age as seen from Figure 5.1. From the three-dimensional plots shown below, it is possible to identify the combination of n and M_s values that result in desirable compressive strengths. The compressive strengths at all ages are found to increase when the n value is increased from 0.03 to 0.05. Activation of slag by alkalis is dependent on the efficiency of the alkalis in solubilizing the silica and alumina from slag [Fernandez et al 1999, Song et al 2000]. Higher alkalinity, i.e., the higher amounts of OH^- ions in solution, results in increased dissociation of the Si along with the liberation of Ca, and thus increased potential for the formation of more amounts of strength imparting reaction products (C-(A)-S-H gel in this case). At a lower n value (0.03), the compressive strengths are quite independent of the M_s values of the activator. Additional Si from waterglass does not facilitate formation of more reaction products when the alkalinity is lower, leading to this observation. When the n value is increased from 0.05 to 0.075, there is a strength reduction that is observed, except for the mixtures with M_s of 1.0 (higher alkalinity). This can be attributed to the leaching of alkalis from the system, that leads to increased porosity, when the amount of alkalis present in the system is more than the optimal range which is reported to be 5.5% (n = 0.055) for pure slag [Wang et al. 1994]. A qualitative evidence of leaching in such cases is presented later.
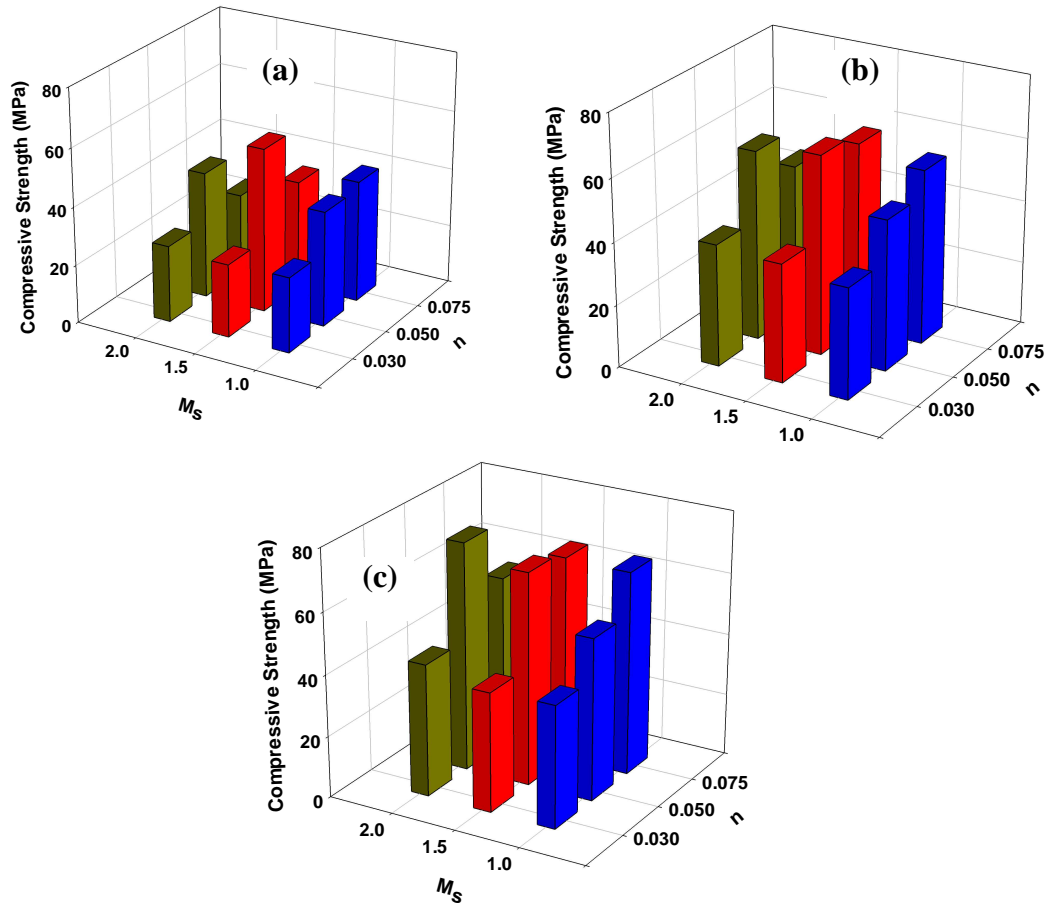
Figure 5.1: Compressive Strength of 100% Slag (a) 3d, (b) 14d and (c) 28d

The impact of leaching and hence the strength loss is found to be generally higher

for the mixtures made using a higher activator M_s and a higher n value [Garcia et

al 2006]. This is because of the formation of a low Ca/Si ratio C-S-H gel as

reported for alkali activated slag systems [Palacios and Puertas 2006, Fernández-

Jiménez et al. 2003] results in the excess silica and alkalis in higher M_s and higher

n value mixtures leaching out under moist curing conditions. At lower M_s (lower

SiO_2 content), strength increases with increasing n values because the higher

alkalinity facilitates the faster formation of reaction products, and the available silica is incorporated into the reaction products. For the higher M_s value (1.5 and 2) mixtures, the results shown here also confirm the presence of an optimal value for n (0.05) as reported in [Wang et al. 1994] as far as compressive strength is concerned.

5.1.2 Influence of moist curing, binder composition and activators on the compressive strength of fly ash-slag blended mortars

Figure 5.2 shows that compressive strength decreases with an increase in the fly ash content for the blended mortars even with higher n values, which is attributable to the poor reactivity of fly ash under ambient conditions.
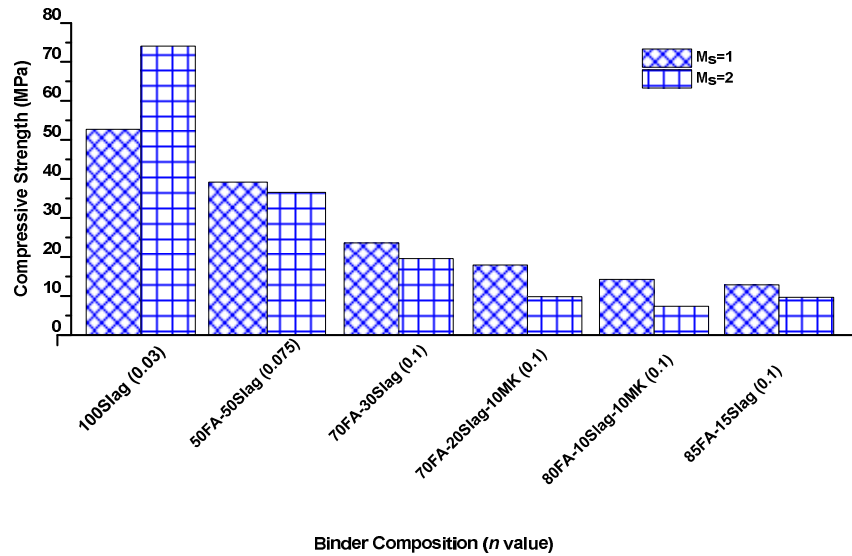
Figure 5.2: Compressive strength of fly ash-slag blends (28d of moist curing)

The decrease in compressive strength with increase in fly ash content is mainly because of the presence of lower amounts of reactive glassy phases in fly ash as compared to slag [Garcia et al 2006, Paloma et al 1999, Van Jaarsveld et al 1997, Vargas et al 2011]. Higher temperature or highly alkaline solutions are required to dissolve the glassy phases in fly ash to form reaction products that provide acceptable compressive strengths. The compressive strength development of 50% fly ash – 50% slag, and 70% fly ash – 30% slag blends are shown in Figure 5.3. The n and M_s values used to prepare these activated blends have been given earlier in Table 4.2.
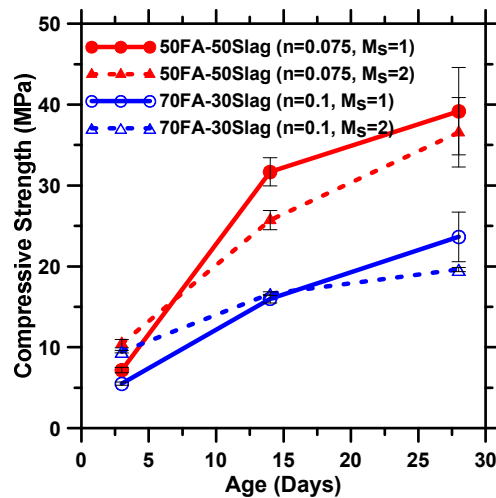
Figure 5.3: Compressive strength of fly ash-slag blends at different ages

Figure 5.3 also shows that the compressive strength of 70% fly ash - 30% slag mortars is lower than those of the 50% fly ash - 50% slag mortars even when activated with 25% more alkalis. Some amount of strength imparting C-S-H gel is formed and some fly ash has reacted to provide a slightly higher increase in reaction product volume in the case of the 70% fly ash - 30% slag mixture.

However the amount of reaction products is lower than that in the 50% fly ash - 50% slag system where a higher amount of slag results in more C-S-H gel formation even at a lower activator alkalinity. In the case of fly ash rich blends the alkali modulus must be kept preferably low ($M_s = 1$) to provide a sufficiently high pH and also to avoid rapid polymerization of the sodium silicate after the pH is reduced by the dissolution of the acidic species in fly ash. If this condition is not satisfied, the matrix would densify before sufficient amounts of reaction products are formed [Garcia et al 2006]. Such initial reaction products would act as a barrier for further progress of the reaction and set the process into diffusion-controlled mode too early. Hence the compressive strength of fly ash rich blends with selected n values is higher for mixtures with lower M_s after 28 days of moist curing. 50% fly ash-50% slag blends n value of 0.075 provides reasonable compressive strengths (>30 MPa) after 28 days of moist curing. The 70%fly ash-30%Slag blends with an n value of 0.1 also provides reasonable strength (23 MPa) for lower silicate modulus (M_s=1) after 28 days of moist curing.

5.1.3   Influence of curing conditions on the compressive strength of slag mortars

Optimal n value of 0.05 determined for the waterglass activated slag systems through the previous section is used to determine the influence of curing conditions on the compressive strength of activated slag systems. The study is conducted by considering two different curing conditions in addition to moist curing (during the entire curing period) that was previously determined. Mortars

were heat cured at 65°C for (a) 6h and (b) 12h in an oven. Once heat curing is completed the cubes were cooled to room temperature and then subjected to moist curing for 14 days and then tested for compressive strength. The compressive strength obtained using these methods are compared to the compressive strength of the cubes that were kept under moist curing for the entire curing period of 14 days. Figure 5.4 shows the influence of curing conditions on the compressive strength of slag mortars. It is known that the early age strength is generally high under heat curing for alkali activated slag systems because of the increased tendency to form the reaction products. Hence the initial period is used for heat curing (6 hrs and 12 hrs). It is found that strength at 14 days of moist curing is higher than those initially exposed to heat (at 65°C). The structure of the reaction product (C-S-H with low Ca/Si ratio) formed due to initial heat curing undergoes modification when it is subjected to moisture thereby reducing its strength.
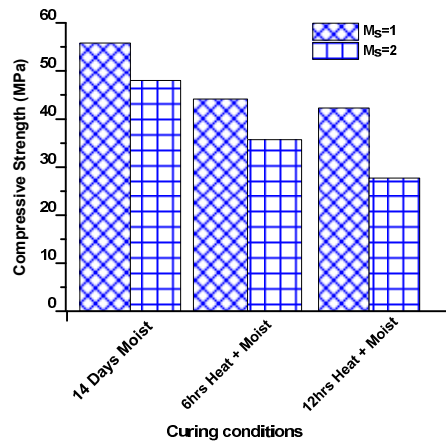
Figure 5.4: Influence of curing conditions on the strength of slag mortars

5.2 Quantification of Leaching through Electrical Solution Conductivity

5.2.1 Effect of leaching on the electrical solution conductivity

68

Electrical conductivity measurements of the deionized water in which the alkali activated specimens were stored for several days were conducted in order to provide a qualitative indication of leaching. The reason behind conducting this experiment is to account for the strength reduction that is observed in the case of activated slag with higher alkali content. The mixes with n values higher than 0.05 in the case of activated slag are more susceptible to leaching when the alkali content increases more than the optimal value as described before. The results are shown in Figure 5.5 (a).
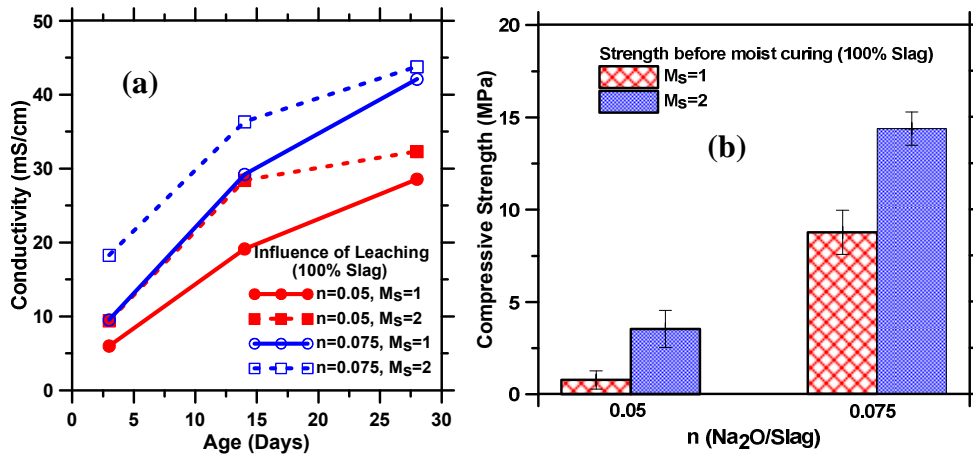
Figure 5.5: (a) Influence of leaching (for n=0.075) on conductivity contributing to reduction in compressive strength of alkali activated slag specimens (b) Strength of 100% slag before subjected to moist curing shows higher strengths for high n and Ms values

The specimens made using higher n and M_s valued solutions exhibited higher conductivities. The solution conductivity is primarily dependent on the concentration of OH- ions (equivalent conductivity of 198 cm^2 S/mol), Na^+ ions (equivalent conductivity of 50.1 cm^2 S/mol) and aqueous SiO_2 (equivalent conductivity of 70 cm^2 S/mol) [Ravikumar and Neithalath 2012, Shebl et al 1987, Snyder et al 2003]. For a paste made using a given n value, the conductivities are

69

higher for the solutions with higher Ms values. This implies a higher amount of SiO_2 in the solution (assuming that similar n values result in similar amount of Na^+ and OH^- ions). Leaching of silica with the solution could result in the removal of silica from the reaction products to achieve local equilibrium, thus contributing to the observed strength reduction at higher n and M_s values when moist cured. Figure 5.5 (b) presents the compressive strengths of these mixtures before they were subjected to moist curing, which shows that the higher n and M_s value mixtures have higher strengths. Though an accurate quantification of leaching cannot be obtained from these measurements, the reasons for the strength reduction in mixtures with higher n and M_s values, stored in high RH conditions, can be garnered from this observation.

5.3 Reaction Product in Activated Slag and Fly ash – Slag Pastes

The preceding sections have dealt with the analysis of the influence of the curing duration, binder composition and activator parameters (n and M_s) on the compressive strengths of activated slag and fly ash-slag mortars. Since the binders, alkali content and the composition of the activating agent influence the reaction product formation, a detailed analysis is attempted in this section. Attenuated Total Reflectance – Fourier Transform Infrared Spectroscopy (ATR-FTIR) is used to obtain information about the reaction products.

5.3.1   FTIR Analysis of activated slag pastes

It is observed that the type of activator plays an important role in the formation of reaction product in the case of alkali activated slag [Fernandez-Jimenez and Puertas 2003]. It is known that activation of slag with sodium silicate results in the formation of C-S-H and C-A-S-H gel as the major reaction product [Wang and Scrivener 1995, Yip et al. 2005, Song et al. 2000]. The discussions here are mostly limited to the stretching vibrations of Si-O-Si units since it can be used as a signature of the main reaction products. In general, for C-S-H and C-A-S-H systems, the Si-O-Si stretching bands are observed at a wavenumber of 950-1000 cm^{-1} [Lodeiro et al. 2008, 2009, Bernal et al. 2011, Palomo et al. 2007]. Figure 5.6 shows the ATR-FTIR spectra of the starting slag showing one broad component at 928 cm^{-1} recognized as (Si-O) stretching of SiO_4 tetrahedra [Fernández-Jiménez and Puertas F 2003]. In the waterglass activated slag pastes the major bands representing the asymmetric stretching vibrations of the silica tetrahedral (Si-O) has been shifted towards higher values (940-960) cm^{-1}. Figures 5.7(a) and (b) represent the 3 and 28 day ATR-FTIR spectra of waterglass activated slag pastes with n values of 0.05 and 0.075 respectively, for M_s values of 1 and 2. The observed shifts can be ascribed to the formation of more condensed tetrahedral species. The FTIR spectra also display bands of calcite (C-O) at 1370-1400 cm^{-1} at lower silicate modulus values. These bands are generally absent at higher silicate modulus indicating less carbonation. Stretching and bending modes of OH^- groups existing in H_2O and in the hydration products were

71

detected at 3320-3365cm^{-1} and also at 1630-1655 cm^{-1}. Calcium hydroxide (CH) band (at ~3635 cm^{-1}) is absent as CH cannot precipitate in these systems because of its higher solubility as compared to C-S-H and C-A-S-H. In general, a move to a higher wavenumber is interpreted as the influence of higher Si content in the C-S-H gel (or a lower Ca/Si ratio) [Palacios and Puertas 2006]. Hence the pastes with a higher M_s value (in this case more SiO_2 was present because more waterglass used to increase the M_s value) shows characteristic signatures shifting to higher wave numbers, as shown in Figure 5.6(b). This is more prominent with increase in reaction time.
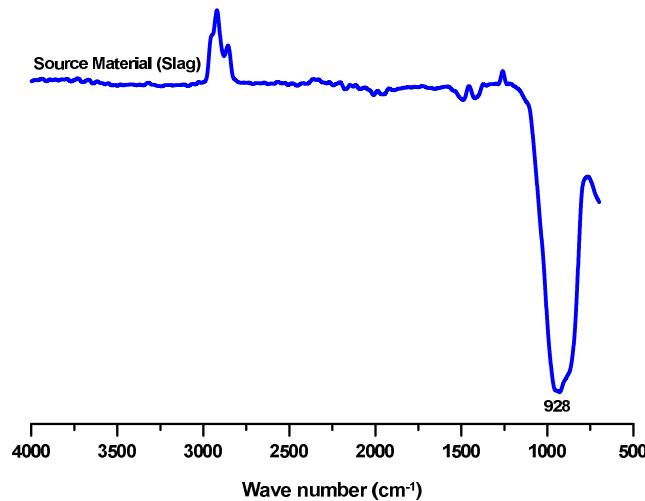
Figure 5.6: ATR-FTIR spectra of source slag

The solubility of Si increases with increase in alkalinity whereas that of Ca decreases and hence the systems with a high silica concentration (higher M_s-value with increasing waterglass) will have a C-S-H gel with a lower Ca/Si ratio. Studies also show that in alkali activated systems containing NaOH the amount of

aluminium incorporated into the tetrahedral chains is high [Fernández-Jiménez et al. 2003], resulting in the Si-O-Si vibration band shifting to higher wavenumbers [Brough and Atkinson 2002] This can be interpreted to be the formation of a more polymerized gel structure [Ravikumar and Neithalath, 2012]. Higher Si content results in the production of Q^3 silicon [Fernandez Jimenez et al. 2003], as opposed to the Q^1 and Q^2 units primarily found in C-S-H from OPC pastes [Schneider et al. 2001]. High presence of Q^2 and Q^3 silicates have been observed in the C-S-H formed in waterglass and NaOH activated slag systems [Puertas et al. 2004, Palacios and Puertas 2006,]. From the figures 5.8 (a) and (b) it can also be inferred that the observed shift in the stretching Si-O-Si band increases with curing duration (3 and 28 days), indicating high silica polymerization with curing time for n value of 0.05. However with an n value of 0.075 the wavenumber decreases with reaction time. This can be related to the increase in the Ca/Si ratio due to leaching of Si. (as seen from compressive strength and electrical solution conductivity results).

(a)

M_S=1

M_S=2

28 Days

3 Days

28 Days

3 Days

3352

3357

1639

1378

1654

1396

942

3352

3363

1642

1642

941

951

939

Wave number (cm^{-1})
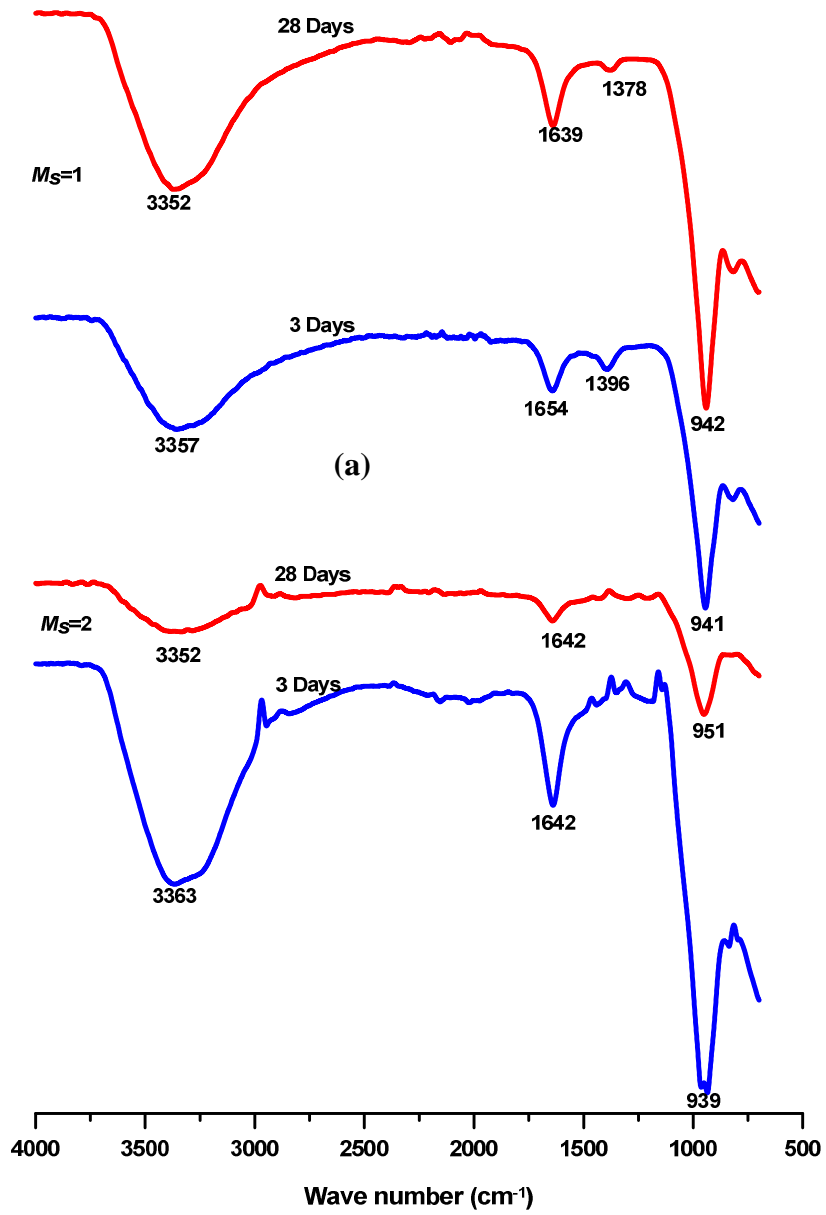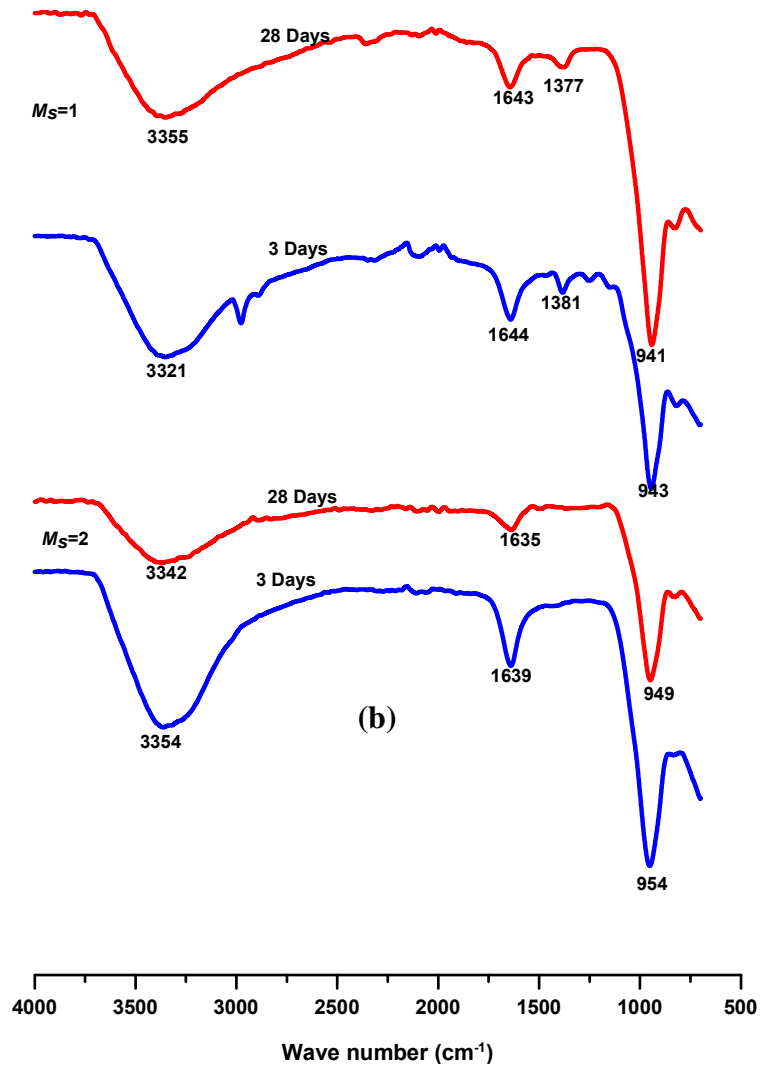
Figure 5.7: ATR-FTIR spectra of waterglass activated slag pastes at 3 and 28 days: (a) n value of 0.05 and (b) n value of 0.075

5.3.2 FTIR Analysis of activated fly ash-slag pastes

The ATR-FTIR analysis of 50% fly ash–50% slag, and 70% fly ash–30% slag blends are shown in Figures 5.8 (a) and (b). The n values used to prepare these activated blends have been given earlier in Table 4.2 with two M_s values (1 and

2). The main Si-O stretching band occurs in the (945-975) cm^{-1} range. The high wave number is contributed by the reaction product having a much lower Ca/Si ratio when compared to that of activated slag paste. The alkaline activation of fly ashes leads to the formation of an alkaline aluminosilicate (N-A-S-H when NaOH is used) of amorphous nature and 3D network, of a zeolitic type.
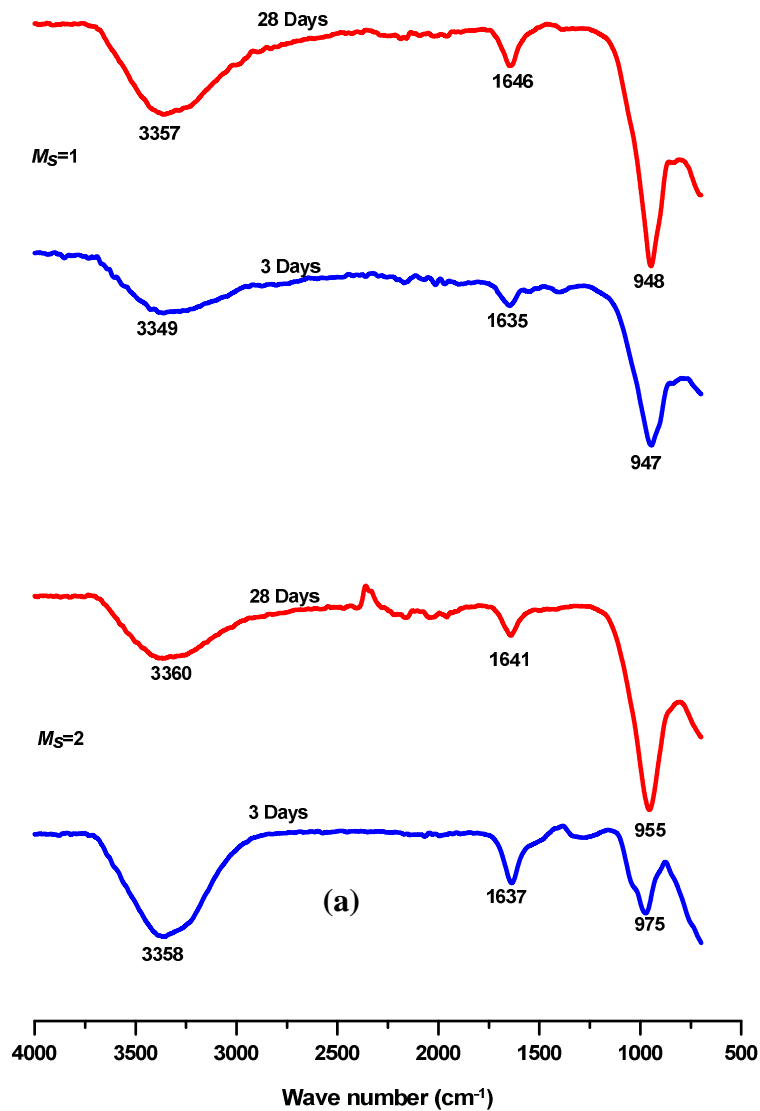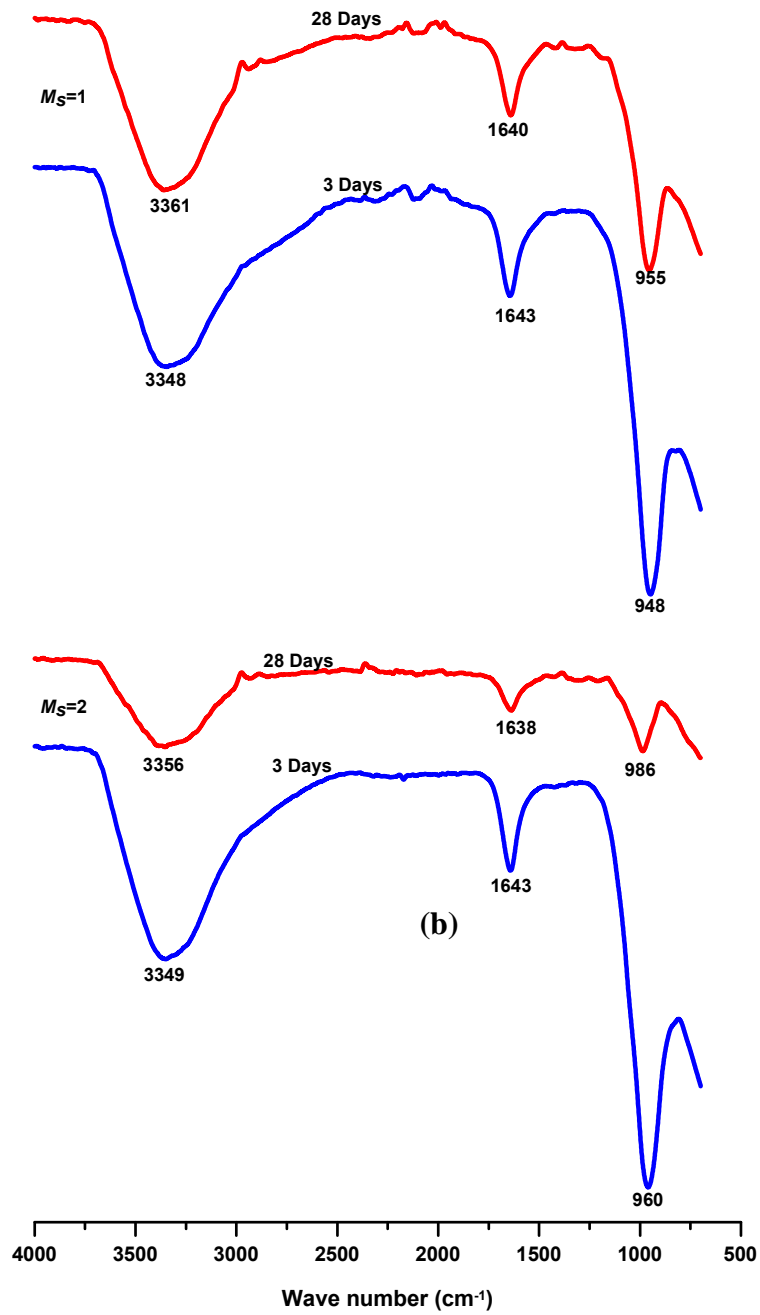
Figure 5.8: ATR-FTIR spectra of waterglass activated fly ash-slag pastes at 3 and 28 days: (a) 50% fly ash-50% slag (n value of 0.075) and (b) 70% fly ash-30% slag (n value of 0.1)

The FTIR spectrum of the alkaline aluminosilicate has a band associated to (Si-O-Si) at 997 cm-1 [Puertas et al, 2000] these are not observed in the IR spectra of

the fly ash–slag pastes studied. This shows the influence of calcium bearing slag in the reaction product (C-S-H) formation. A high silicate modulus of the activator (M_s) results in a shift to a higher wavenumber both at early (3 days) as well as later (28 days) ages. The calcite peak (C-O) which is predominant in slag pastes at 1400 cm^{-1} is absent in fly ash rich blends indicating reduced carbonation with increase in fly ash content. Stretching and bending modes of OH^- groups existing in H_2O and in the hydration products were detected at 3320-3365cm^{-1} and also at 1630-1655 cm^{-1} similar to slag pastes.

5.3.3 Reaction products and compressive strength

As a consequence of the alkaline activation of slag paste, a hydrated calcium silicate of the C-S-H gel type is formed as the main reaction product. This gel phase is differentiated from that formed in the hydration of Portland cement because of its lower Ca/Si molar ratio. The higher Na proportion in solution due to the addition of NaOH would favour the formation of C-S-H gel. Sodium will enter the structure in inter-layer spaces [Puertas et al, 2000] and acts as a catalyst for the formation of C-S-H. Hence the mixes made with high alkalinity (high n values) has high compressive strengths. NaOH added to modify the M_s value changes the number of network modifying Na atoms per Si atom [Ravikumar and Neithalath, 2012]. The structure of the silicate phases formed is modified by the presence of Na atoms [Dimas et al. 2009]. The Na ions will be incorporated in the C-S-H gel by replacing Ca ions. It acts as charge balancers for the negative charge

on the Al tetrahedral [Fernández-Jiménez et al. 2003, Shi et al. 2007, Ravikumar and Neithalath, 2012].

Higher silicate modulus leads to high silica polymerization. This is due to the formation of Q^3 silicate structures with high silicate modulus resulting in decreased number of non-bridging oxygen sites [Dimas et al. 2009]. The formation of Q^3 silicate structures results in higher wavenumber corresponds to the asymmetric stretching vibration of the silica tetrahedral. Hence for the slag pastes with optimal alkalinity (n=0.05) strengths are higher for mixes with high silicate modulus at later age (28 days).

5.4 Influence of Curing Conditions on Heat Cured Fly Ash Mortars

5.4.1   *Compressive strength development*

As mentioned before the activation of fly ash with alkalis requires heat curing to gain reasonable mechanical properties because of the poor reactivity of the fly ash at ambient temperature. Given that our objective is to identify fly ash rich blends for moist curing it is important to identify the compressive strength development of the heat cured fly for comparison. Since fly ash mixes do not reach their initial set with a liquid-to-powder ratio of 0.5 a liquid-to-powder ratio of 0.4 is used to identify the compressive strength development of fly ash mixes with heat curing. The influence of curing conditions on the compressive strength improvement of heat cured fly ash mortars are studied by considering three different types of heat curing procedures.

79

Method 1: (Open dry condition): The mortar cubes were placed directly in an oven at 75°C. Method 2: (Open moist condition): The mortar cubes were placed in the oven at 75°C alongside a container containing water (relative humidity 40–50%). Method 3: (Closed condition):
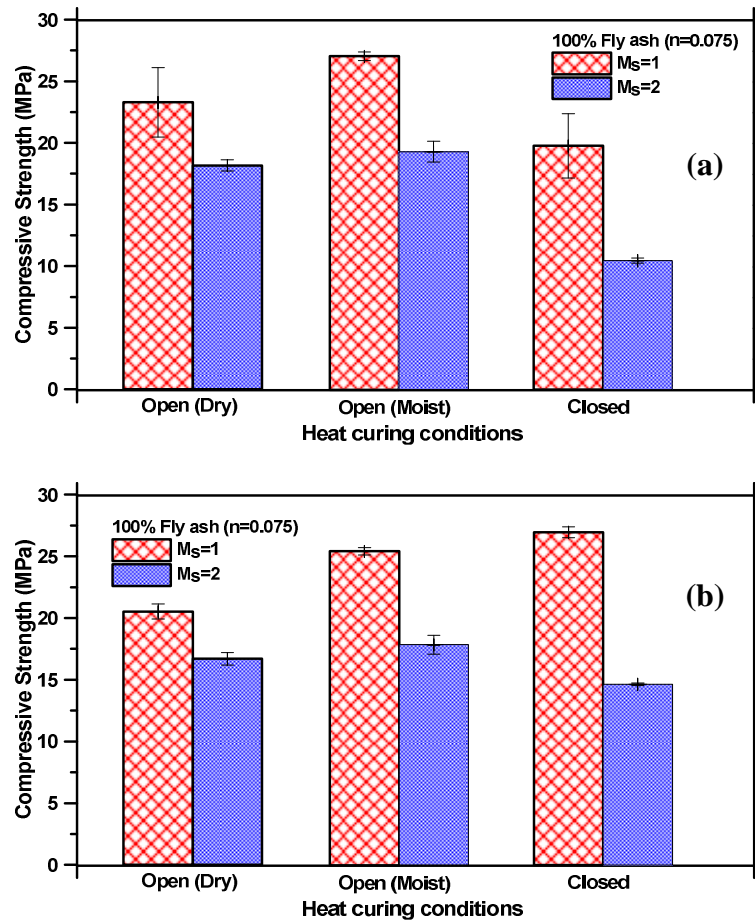
Figure 5.9: Influence of heat curing (at 75C) conditions on the compressive strength development of fly ash mixes after (a) 24 hours and (b) 48 hours

The mortar cubes were sealed with aluminium foil. The cubes were then placed in an oven at 75°C. The compressive strength development shows that with an n

80

value of 0.075, activated fly ash mixtures can attain appreciable strength (>20 MPa) with a liquid-to-powder ratio of 0.4. Figure 5.9 (a) shows that after 24 hours the strength of fly ash mortar cubes cured by means of Method 2 (Open moist) is higher than that of Method 1 (Open Dry) and Method 3. However with time, the compressive strength of mortars cured using Method 1 and 2 (Open) decreases due to increased porosity with loss of water causing drying shrinkage over time. After 24 h, the Method 3 (closed) cured fly ash had a generally porous matrix and hence its strength is lesser when compared to that of the strength of mortars obtained using other curing methods (1 and 2). However the primary reaction product, N–A–S–H gel, enriches in silicon content over time and gains reasonable strength, as depicted in Figure 5.9 (b). Hence, with closed curing conditions, the curing time proved to be an essential factor in the acquisition of mechanical properties and favors the formation of small zeolitic crystals [Criado et al, 2010]. By means of closed curing, the excess amount of free water favors the dissolution of the vitreous component of the fly ash, stimulating the activation reaction and yielding a well developed material, with high strength over time. This suggests the influence of curing duration on the compressive strength development when cured using Method 3. Closed heat curing yields a dense, compact material, whose initially high aluminum content gives way to silicon uptake and good mechanical property development over time. Open heat curing with the pastes in direct contact with the atmosphere generates a granular, porous material. The aluminium-rich reaction products are very stable, with a chemical composition

that remains unchanged throughout the curing process, ultimately resulting in a weaker material.

5.4.2 *FTIR analysis of the activated fly ash pastes*

Figures 5.10 (a) and (b) shows the influence of heat curing conditions on the FTIR spectra of fly ash mixes. The main band in fly ash mixes are shifted to higher wavenumber (988-1008 cm^{-1}) corresponding to alkaline alumino silicate band (N-A-S-H gel in this case) [Criado et al. 2010]. The stretching vibrations of Si-O-Si of closed cured mixes after 48 hours of heat curing shows a higher wavenumber compared to that of the pastes cured in open conditions. This is indicative of changes in the Si/Al ratio in the major reaction product. With closed curing, as the heat curing time increases, the amount of reaction product formed increases, resulting in a higher wavenumber as compared to open cured pastes. The width of the band observed is larger for closed cured specimens when compared to that of the open cured specimens. A wider distribution of vibrational energies increases the bandwidth in the FTIR spectrum [Ruben et al. 1995]. The broad band observed with closed curing can be interpreted as a change in the structure of the molecular structure during gelation. The additional water present in closed heat cured specimens tends to observe more heat, decreasing the molecular order thereby increasing its band width.
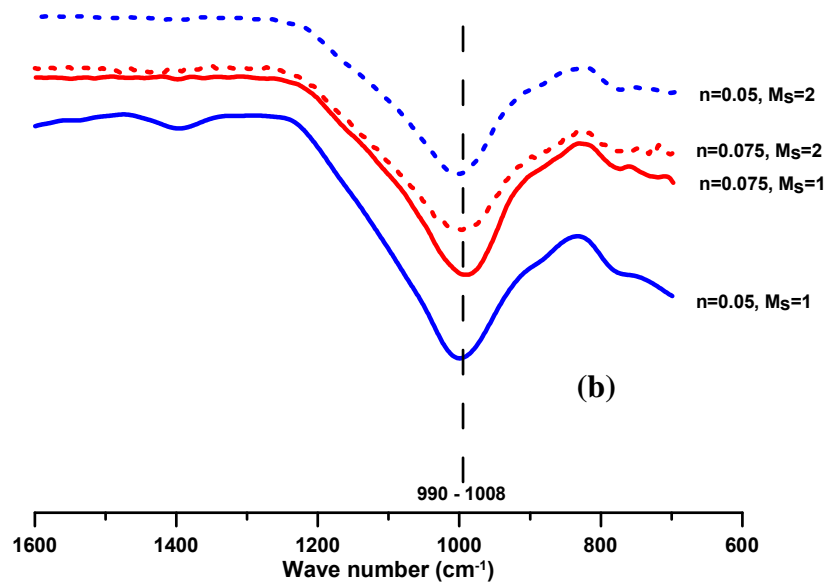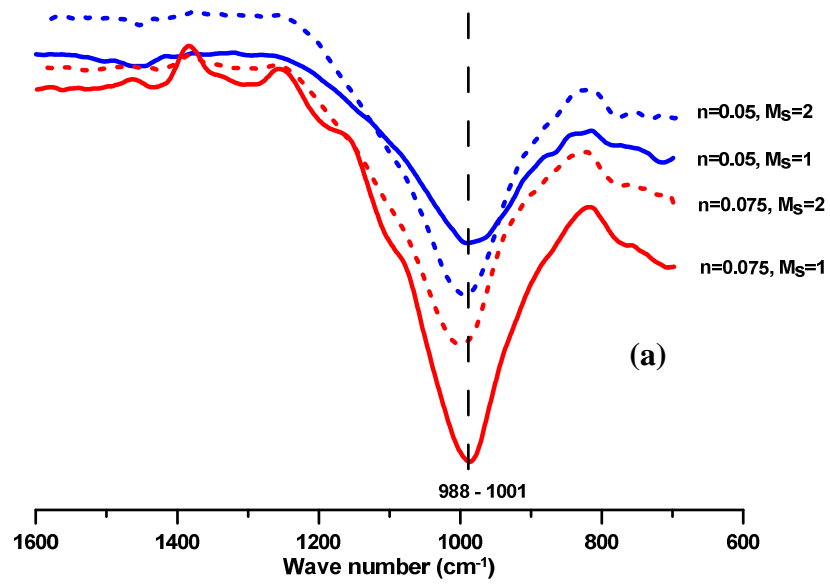
Figure 5.10: Influence of heat curing (at 75C) conditions on the ATR-FTIR spectra of fly ash mixes after 48 hours (a) Open and (b) Closed

5.5 Summary

The influence of moist curing, binder composition and activator concentration on the compressive strength development and reaction product formation of sodium silicate solution activated slag and fly ash-slag blends are discussed in this chapter. An optimal n value of 0.05 is determined for slag mortars. At higher alkali content leaching of alkalis resulting in strength reduction for higher silicate modulus mixes. Electrical conductivity of solutions in which the specimens were stored shows higher conductivity values for high n and high M_s value pastes, which explains the strength reduction of slag mortars for n values of 0.075 at high moduli (1.5 and 2). FTIR analysis helps in determining the reaction products in slag and fly ash-slag blends. The influence of heat curing conditions on the compressive strength development and reaction product formation of fly ash mixes were also reported in this chapter.

6. CONCLUSIONS

6.1 Early Age Response of Activated Slag and Fly ash – Slag Systems

The major conclusions made based on the early age responses of sodium silicate activated slag and fly ash-slag blends are the following

- The maximum fly ash content that can be used in fly ash-slag blends to obtain desirable setting is 70%. Higher n values are required when the amount of slag in the fly ash-slag blended mixtures is reduced.

- The minimum n values at which desirable initial setting is obtained for the mixtures are 0.03 for 100% slag, 0.05 for 50%fly ash–50%Slag, and 0.1 for 70%fly ash – 30%Slag.

- In waterglass activated slag and fly ash-slag blends increase in activator M_s (from 1 to 2) results in a much larger impact on setting times. The mixtures with lower n and higher M_s values set faster than the mixtures with higher n and lower M_s values. This trend is observed irrespective of binder composition.

- A comparative analysis of the reaction kinetics in waterglass activated slag and fly ash rich blended systems determined using isothermal calorimetry is presented. For the pastes activated using waterglass, the response was observed to be similar to that of OPC hydration. However the induction period in waterglass activated slag paste is found to be considerably longer than that of the OPC paste. The induction period can be shortened with increase in alkalinity (by increasing the n value or decreasing the M_s value). The

waterglass activated slag pastes also have a much smaller acceleration peak when compared to that of OPC.

- The waterglass activated fly ash-slag systems show only one large peak that is generally observed within the first 2-3 hours. The only exception is the 50% fly ash-50% slag blend with M_s of 1 (higher alkalinity) that demonstrates a broader, low intensity peak after 20 hours.

- The maximum cumulative heat release (at 40°C) after 72 hours in waterglass activated systems is observed for slag pastes (190 J/g). However it is lower than that of OPC (310 J/g) at the same temperature.

- Increase in temperature has a profound effect on the heat release rates for the fly ash rich blends. Kinetic modeling of the alkali activation reaction of waterglass activated slag and fly ash-slag systems has been carried out to quantify the differences in reaction kinetics using exponential as well as Knudsen method. The constant K determined using the Knudsen method is considered as a rate determining parameter in the case of activated slag and cement (when the difference in the Q_{max} values are not very large with increase in temperature) however it cannot be considered as a rate determining parameter in the case of fly ash rich blends (since the difference in the Q_{max} values are very large with temperature especially from 25°C to 35°C). The activation energy determined using rate constant values (based on Arrhenius law) are found to be higher for activated slag (56.7 KJ/mol) when compared to that of cement (46.8 KJ/mol).

6.2 Compressive Strength and Reaction Products of Activated Slag and Fly ash –
Slag Systems

The main conclusions drawn based on the compressive strength and reaction
product analysis of slag and fly ash-slag blends are the following

- Very high compressive strengths are obtained both at early ages as well as later
  ages (more than 70 MPa) with waterglass activated slag mortars.

- Optimal alkali content as expressed by the Na_2O-to-source material ratio (n) in
  the case of waterglass activated slag mortars is found to be closed to 0.05
  based on the experiments. Beyond this ratio, compressive strength decreases
  for high silicate modulus mixes. This is due to leaching of alkalis from the
  system when the amount of alkalis present in the system is more than the
  optimal range, which leads to increased porosity.

- A qualitative evidence of leaching is presented by conducting electrical
  solution conductivity. The impact of leaching and the strength loss is found to
  be generally higher for the mixtures made using a higher activator M_s and a
  higher n value.

- Compressive strength decreases with the increase in the fly ash content.
  Increasing alkalinity of the activator facilitates production of moist cured fly
  ash rich blends with compressive strengths in the 20 MPa range.

- Attenuated Total Reflectance – Fourier Transform Infrared Spectroscopy
  (ATR-FTIR) is used to obtain information about the reaction products. In the
  waterglass activated slag pastes the major bands representing the asymmetric

stretching vibrations of the silica tetrahedral (Si-O-Si) has been shifted towards higher values (940-960) cm^{-1} corresponding to C-S-H gel. Slag and fly ash-slag pastes with a higher M_s value shows C-S-H peak shifting to higher wave numbers. The alkaline activation of fly ash-slag blends also shows only one peak but at a higher wavenumber representing the formation of an alkaline aluminosilicate (N-A-S-H when NaOH is used) of amorphous nature and 3D network, of a zeolitic type. The FTIR spectrum characteristic of the alkaline aluminosilicate (SiO) at 997 cm-1 [Puertas et al, 2000] are not observed in the IR spectra of the fly ash–slag pastes studied showing the influence of calcium bearing slag in the reaction product (C-S-H) formation of fly ash-slag blends.

- Closed heat curing yields a dense, compact material, whose initially high-aluminium content gives way to good mechanical development over time. Open heat curing with the pastes in direct contact with the atmosphere generates a granular, porous material.

- The influences of heat curing conditions on the FTIR spectra of fly ash mixes were studied. The main band in fly ash mixes are shifted to higher wavenumber (988-1008) corresponding to alkaline alumino silicate band. The stretching vibrations of Si-O-Si of closed cured mixes after 48 hours of heat curing shows higher wavenumber compared to that of the pastes cured using in open conditions indicating the changes in the Si/Al ratio in the chief reaction product.

7. REFERENCES

1. ACI 318:2011 Building Code Requirements For Structural Concrete And Commentary

2. ACI Strategic Development Committee, "Concrete Sustainability. A Vision for Sustainable Construction with Concrete in North America", draft v7.3, appendix C, November 14, 2008

3. Bakharev T, Durability of geopolymer materials in sodium and magnesium sulfate solutions, Cement and Concrete Research, 35 (2005) 1233-1246

4. Bakharev T, Geopolymeric materials prepared using Class F fly ash and elevated temperature curing, Cement and Concrete Research 35 (2005) 1224-1232

5. Bakharev T, Sanjayan J.G, Cheng Y.B, Alkali activation of Australian slag cements, Cement and Concrete Research 29 (1999) 113-120

6. Bakharev T, Resistance of geopolymer materials to acid attack, Cement and Concrete Research 35 (2005) 658-670

7. Bernal S.A, de Gutierrez R.M, Pedraza A.L, Provis J.L, Rodriguez E.D, Delvasto S, Effect of binder content on the performance of alkali-activated slag concretes, Cement and Concrete Research 41 (2011) 1-8

8. Bijen J, Waltje H, Alkali activated slag-fly ash cements, Conference on fly ash, Silica Fume, Slag and Natural Pozzolans in Concrete, Trondheim, Norway, 1989.

9. Brough A.R and Atkinson A, Sodium silicate-based, alkali-activated slag mortars: Part I. Strength, hydration and microstructure, Cement and Concrete Research 32 (2002) 865-872

10. Chang J.J, A study on the setting characteristics of sodium silicate-activated slag pastes, Cement and Concrete Research 33 (2003) 1005-1011

11. Chindaprasirt P, Chareerat T, Sirivivatnanon V, Workability and strength of coarse high calcium fly ash geopolymer, Cement and Concrete Composites 29 (2007) 224-229

12. Criado M, Fernández-Jiménez A and Palomo A, Alkali activation of fly ash. Part III: Effect of curing conditions on reaction and its graphical description, Fuel 89 (2010) 3185–3192

13. Davidovits J, Geopolymer chemistry and sustainable development. The Poly (sialate) terminology: a very useful and simple model for the promotion and

understanding of green-chemistry, in: J. Davidovits (Ed), Proceedings of the World Congress Geopolymer, Saint Quentin (France), 2005, 69-73

14. Davidovits. J, Geopolymers: Inorganic Polymeric New Materials, Journal of Thermal Analysis 37 (1991) 1633-1656.

15. Dimas I, Giannopoulou, Panias D, Polymerization in sodium silicate solution: a fundamental process in geopolymerization technology, Journal of Material Science, 44 (2009) 3719-3730

16. Duxson P, Provis J.L, Luckey G.C, Mallicoat S.W, Kriven W.M, van Deventer J.S.J, Understanding the relationship between geopolymer composition, microstructure and mechanical properties, Journal of Colloids and surfaces A: Physiochem.Eng.Aspects 269 (2005) 47-58

17. Fernández-Jiménez, and Criado M, Microstructure development of alkali-activated fly ash cement: a descriptive model, Cement and concrete research 35 (2004) 1204-1209

18. Fernández-Jiménez and Puertas F, Alkali-activated slag cements: Kinetic studies, Cement and Concrete Research 27 (3) (1997) 359-368

19. Fernández-Jiménez and Puertas F Structure of Calcium Silicate Hydrates Formed in Alkaline-Acitvated Slag: Influence of the Type of Alkaline Activator, Journal of American Ceramic Society 86 (2003) 1389-1394

20. Fernández-Jiménez, Palomo J.G, Puertas F, Alkali-activated slag mortars: Mechanical strength behavior, Cement Concr. Res 29 (1999) 1313-1321

21. Fernandez-Jimenez A, Palomo A, Composition and microstructure of alkali activated fly ash binder: effect of the activator. Cement and Concrete Research 35 (2005) 1984–1992.

22. Fernandez-Jimenez A. and Puertas F., 2001, "Setting of alkali-activated slagcement. Influence of activator nature" Adv. Cem. Res. 13 (3), pp.115-121.

23. Fernandez-Jimenez A., Paloma A., 2003, "Characterisation of fly ashes. Potential reactivity as alkaline cements", Fuel 82 (18), pp.2259-2265.

24. Garcia J.I.E, K. Campos-Venegas, A. Gorokhovsky and A. Fernandez, Cementitious composites of pulverised fuel ash and blast furnace slag activated by sodium silicate: effect of Na_2O concentration and modulus, Advances in applied ceramics (2006) 105–4.

25. Gerstig M and Wadso L, A method based on isothermal calorimetry to quantify the influence of moisture on the hydration rate of young cement pastes, Cement and Concrete Research, 40 (6) (2010) 867-874

26. Glasser F.P., 1990, "cements from micro to macrostructure" Br. Ceram. Trans. J. Vol.89, nº 6, pp.192-202

27. Glifford P.M, Gillot J.E, Behaviour of mortar and concrete made with activated blast furnace slag cement, Canadian Journal of Civil Engineering, 24 (2) (1997) 237-249

28. Glukhovsky, V. D., 1965, Soil Silicates, Their Properties, Technology of Manufacturing and Fields of Application, Doct. Tech. Sc. Degree Thesis, Kiev Civil Engineering Institute, Kiev, USSR.

29. Glukhovsky V., 1994, Frist. Inter.Conf. Alkaline Cements and Concretes. 1, pp.1-8. Kiev. Ukraine

30. Gong C and Yang N, Effect of phosphate on the hydration of alkali activated red mud-slag cementitious material, Cement and Concrete Research 30 (7) (2000) 1013-1016

31. Guerrieri M, Sanjayan G, Behavior of combined fly ash-slag-based geopolymers when exposed to high temperatures, Fire and Materials 34(2010) 163–175.

32. Hardjito D and Rangan B.V, Development and properties of low-calcium fly ash-based geopolymer concrete, Curtin Research Report, http://www.geopolymer.org/library/technical-papers/17-development-and-properties-of-low-calcium-fly-ash-based-geopolymer-concrete

33. Hong S.Y and Glasser F.P, Alkali sorption by C-S-H and C-A-S-H gels: Part II. Role of alumina, Cement and Concrete Research 32 (2002) 1101-1111

34. I-Cal 8000 Isothermal calorimeter for concrete and cement, User manual, Calmetrix Inc.

35. Knudsen, T., 1980, On particle size distribution in cement hydration. 7th International Congress on the Chemistry of Cement, Paris, France, II, 170–175.

36. Kong D.L.Y and Sanjayan J.G, Damage behavior of geopolymer composites exposed to elevated temperatures, Cement and Concrete Composites 30 (2008) 986-991

37. Krivenko P.D, Alkaline cements, Paper presented at the first international conference on alkaline cement and concretes, Kiev, Ukarine (1994)

38. Krizan D and Zivanovic B, Effects of dosage and modulus of water glass on early hydration of alkali-slag cements, Cement and Concrete Research 32 (2001) 1181-1188

91

39. Lodeiro I.G, Fernández-Jiménez A, Blanco M.T, Palomo A, FTIR study of sol-gel synthesis of cementitious gels: C-S-H and N-A-S-H, Journal of Sol-Gel science and technology, 45 (2008) 63-72

40. Lodeiro L.G, D.E. Macphee, A. Palomo and A. Fernández-Jiménez, Effect of Alkalis on Fresh C-S-H Gels. FTIR Analysis, Cement and Concrete Research 39 (2009) 147-53

41. Mehta P.K, Sustainability of the Concrete Industry – Critical Issues, ACI Strategic Development Committee's "Concrete Summit on Sustainable Development", March 29, 2007, Washington DC CO_2 emission

42. Mitchell L.D, J.C Margeson, J.J. Beaudoin, Synthesis and characterisation of lithium and sodium doped C-S-H, 12th International Congress on the Chemistry of Cement, Montreal, July 8-13, (2007) 1-17

43. Neithalath N, Quantifying the effects of hydration enhancement and dilution in cement pastes containing coarse glass powder, 6 (1) (2008) 1-12

44. Palacios M and F. Puertas, Effect of Carbonation on Alkali-Activated Slag Paste, Journal of American Ceramic Society 89 (2006) 3211-3221.

45. Paloma A, and de la Fuente J.I.L, Alkali-activated cementitious materials: Alter Cement and Concrete Composites native matrices for the immobilization of hazard Cement and Concrete Composites ous wastes Part I. Stabilisation of boron, Cement and Concrete Research 33 (2003) 28 Cement and Concrete Composites 1-288.

46. Palomo A, Fernández-Jiménez, Kovalchuk G, Ordonez L.M, Naranjo M.C, OPC-fly ash cementitious systems: study of gel binders produced during alkaline hydration, Journal of Material Science 42 (2007) 2958-2966

47. Palomo, J.I.L. de la Fuente, Alkali-activated cementitious materials: Alternative matrices for the immobilization of hazardous wastes Part I. Stabilisation of boron, Cement and Concrete Research 33 (2003) 281-288

48. Provis J.L and van Deventer J.S.J, Geopolymerisation kinetics. 2. Reaction kinetic modeling, Chemical Engineering Science 62 (2007) 2318-2329

49. Puertas F, Fernández-Jiménez A, Blanco-Varela M.T, Pore solution in alkali-activated slag cement pastes. Relation to the composition and structure of calcium silicate hydrate, Cement and Concrete Research, 34 (2004) 195–206

50. Puertas F, Fernandez-Jimenez A, Mineralogical and micro-structural characterization of alkaliactivated fly ash-slag cement, Cement Concrete Composites 25 (2003) 287–292.

92

51. Puertas F, Martinez-Ramirez S, Alonso S, Vazquez T, Alkali activated fly ash/slag cement, strength behaviour and hydration products, Cement and Concrete Research 30 (2000) 1625-1632.

52. Purdon, A. O., 1940, The action of alkalis on blast-furnace slag. Journal of the Society of Chemical Industry, 59, 191–202.

53. Ravikumar D, Property development, microstructure and performance of alkali activated fly ash and slag systems, Ph.D. Thesis, Clarkson University, 2012, pp. 1–217.

54. Ravikumar D Peethamparan S, and Neithalath N. ―Structure and strength of NaOH activated concretes containing fly ash or GGBFS as the sole binder, Cement and Concrete Composites 32 (2010) 399-410

55. Ravikumar D and Neithalath N - Reaction kinetics in sodium silicate powder and liquid activated slag binders evaluated using isothermal calorimetry, Thermochimica Acta 546 (2012) 32– 43

56. Ravikumar D and Neithalath N ―The effects of alkali content on the reaction products in alkali silicate powder activated slag binders□, under review with Cement and Concrete Composites

57. Roy, D. M. and Idorn, G. M., 1982, Hydration, structure, and properties of blast furnace slag cements, mortars and concretes. ACI Journal, 79(6), 444–456.

58. Roy, D. M. and Idorn, G. M., 1985, Relationships between strength, pore structure and associated properties of slag-containing cementitious materials. Materials Research Society Symposium, 42, 133–142.

59. Rubensa P, Snauwaerta J, Heremansa K, Stuteb R, In situ observation of pressure-induced gelation of starches studied with FTIR in the diamond anvil cell, Carbohydrate Polymers 39 (1999), 231–235.

60. Schindler A.K, K.J. Folliard, Heat of hydration models for Cementitious Materials, ACI Material Journal, 102 (1) (2005) 24-33

61. Shebl F.A, Summan A.B and Helmy F.M, Conductance of tricalcium silicate in water, Cement and Concrete Research Vol. 18, pp. 121-130, 1988.

62. Shi, C. and Li, Y., 1989a, Effect of the modulus of water glass on the activation of phosphorus slag. Il Cemento, 86(3), 161–168.

63. Shi, C. and Li, Y., 1989b, Investigation on some factors affecting the characteristics of alkali-phosphorus slag cement. Cement and Concrete Research, 19(4), 527–533.

64. Shi C and R. Day, Pozzolanic reaction in the presence of chemical activators: Part II — Reaction products and mechanism, Cement Concr. Res 30 (2000) 607-613

65. Shi C and R. Day, Some factors affecting early hydration of alkali-slag cements, Cement Concr. Res 26 (1996) 439-447

66. Shi C, P.V. Krivenko and D. Roy, Alkali-Activated Cement and Concretes, Taylor and Francis, New York (2006)

67. Shi C, R. L. Day, A calorimetric study of early hydration of alkali-slag cements, Cement and Concrete Research, 25 (6) (1995) 1333-1346

68. Shi C, Strength, Pore structure and permeability of alkali-activated slag mortars, Cement and Concrete Research 26 (1996) 1789-1799

69. Shi C, Day R.L, Early strength development and hydration of alkali - activated blast furnace slag / Fly ash blends, Advances in Cement Research 11 (1999) 189-196.

70. Shi C, Day R.L, Early hydration characteristics of alkali slag cements, Cement and Concrete Research, 25 (1995) 1333-1346.

71. Shi C, Day R.L, Selectivity of alkaline activators for the activation of slags. Cement Concrete Aggregates 18 (1996b) 8–14.

72. Smith M.A, Osborne G.J, Slag / fly ash cements, World Cement Technology 8 (1977) 223-233.

73. Snyder K.A, Feng X, Keen B.D, Mason T.O, Estimating the electrical conductivity of cement paste pore solutions from OH, K^+ and Na^+ concentrations, Cement and Concrete Research 33 (2003) 793–798

74. Song S, Sohn D, Jennings H.M and Mason T.O, Hydration of alkali-activated ground granulated blast furnace slag, Journal of Material Science 35 (2000) 249-257

75. Taylor H.F.W, Cement Chemistry, 2nd Edition, Thomas Telford, London, 1997

76. Tuchbreiter A, Marquardt J, Zimmermann J, Walter P and Mülhaupt R, Highthroughput evaluation of olefin copolymer composition by means of Attenuated Total Reflection Fourier Tranform Infrared Spectroscopy. Journal of Combinatorial Chemistry, 2001. 3(6): p. 598-603.

77. Van Deventer J.S.J, J.L. Provis, P. Duxson, G.C. Lukey, Reaction mechanism in geopolymeric conversion of inorganic waste to useful products, Journal of hazardous Materials A 139 (2007) 506-513

78. Van Jaarsveld J.G.S, Van Deventer J.S.J, G. Lukey, The characterisation of source materials in fly ash-based geopolymers, Materials Letters 57 (2003) 1272–1280

79. Wadso L, An experimental comparison between isothermal calorimetry, semi adiabatic calorimetry and solution calorimetry for the study of cement hydration, final report, NORDTEST project 1534-01 (2003).

80. Wang S.D and Scrivener K.L, 29Si and 27Al NMR study of alkali-activated slag, Cement Concr. Res 33 (2003) 769-774

81. Wang S.D and Scrivener K.L, Hydration products of alkali activated slag cement, Cement Concr. Res 25 (1995) 561-571

82. Wang S.D, Pu X.C, Scrivener K.L, Pratt P.L, Factors affecting the strength of alkali activated slag, Cement and Concrete Research,Vol.24, No. 6,p p. 1033-1043,1994

83. Xu, Hu, Ruiz J M, Wang K, Zhi G, Isothermal calorimetry tests and modeling of cement hydration parameters, Thermochimica Acta 499 (2010) 91–99

84. Yang K.H, J.K. Song, A.F. Ashour, E.T. Lee, Properties of cementless mortars activated by sodium silicate, Construction and Building Materials 22 (2009) 1981-1989

85. Yip C.K, G.C. Lukey, J.S.J. van Deventer, The coexistence of geopolymeric gel and calcium silicate hydrate at the early stage of alkaline activation, Cement and Concrete Research 35 (2005) 1688-1697

86. Yunsheng. Z, Wei S, Qianli C,Lin C, Synthesis and heavy metal immobilization behavior of slag geopolymer, Journal of Hazardous Materials 143 (2007) 206-213

87. Zhao F.Q, Ni W, Wang H.J, Liu H.J, Activated fly ash-slag blended cement, Resources, Conservation and Recycling 52 (2007) 303–313.

88. Zhou, H., Wu, X., Xu, Z. and Tang, M., 1993, Kinetic study on hydration of alkali-activated slag. Cement and Concrete Research, 23(6), 1253–1258.